University of Szeged
Albert Szent-Györgyi Medical School
Doctoral School of Theoretical Medicine

The role of the sigma-1 receptor ligands in the arachidonic acid metabolism of healthy and diabetic rat platelets or abdominal aorta

PhD Thesis

Sándor Váczi M.Sc.

Supervisor: Zsófia Lepránné Mezei, M.D., Ph.D.

Szeged
2023

TABLE OF CONTENTS

SCIENTIFIC PUBLICATIONS ON THE SUBJECT OF THE THESIS

I. Váczi S, Barna L, Harazin A, Mészáros M, Porkoláb G, Zvara Á, Ónody R, Földesi I, Veszelka S, Penke B, Fülöp L, Deli MA, Mezei Z. S1R agonist modulates rat platelet eicosanoid synthesis and aggregation.
Platelets. 2021; 16:1-10. doi: 10.1080/09537104.2021.1981843. PMID: 34697991
IF: 4.236 Q1

II. Váczi S, Barna L, Laczi K, Tömösi F, Rákhely G, Penke B, Fülöp L, Bogár F, Janáky T, Deli MA, Mezei Z. Effects of sub-chronic, *in vivo* administration of sigma non-opioid intracellular receptor 1 ligands on platelet and aortic arachidonate cascade in rats.
Eur J Pharmacol. 2022 Jun 15; 925:174983. doi: 10.1016/j.ejphar.2022.174983. Epub 2022 Apr 27. PMID: 35487254
IF: 5.195 Q1

III. Váczi S, Barna L, Laczi K, Tömösi F, Rákhely G, Penke B, Fülöp L, Bogár F, Janáky T, Deli MA, Mezei Z. Effects of sub-chronic, *in vivo* administration of sigma-1 receptor ligands on platelet and aortic arachidonate cascade in streptozotocin-induced diabetic rats.
PLoS One. 2022 Nov 17; 17 (11):e0265854. doi: 10.1371/journal.pone.0265854. eCollection 2022. PMID: 36395179 Free PMC article.
IF: 3.752 Q1

INTRODUCTION

The sigma-1 receptor (S1R) is expressed in cells in both the central nervous system and peripheral organs. The presence of this receptor has been demonstrated in neurons, glia, endothelial cells and T lymphocytes. S1Rs are mainly located in the mitochondria-associated membrane (MAM) of the endoplasmic reticulum (ER) but are able to migrate from the ER to the plasma membrane [1].

Through translocation and protein-protein interactions, S1Rs are involved in the regulation of intracellular signalling pathways by modulating the activity of ion channels, inositol phosphatases and protein kinases [2–7].

The substrate of eicosanoids, a secondary intracellular signal transducer, is arachidonic acid (AA) released from membrane phospholipids (PL) by phospholipase A_2 (PLA_2) (Fig. 1).

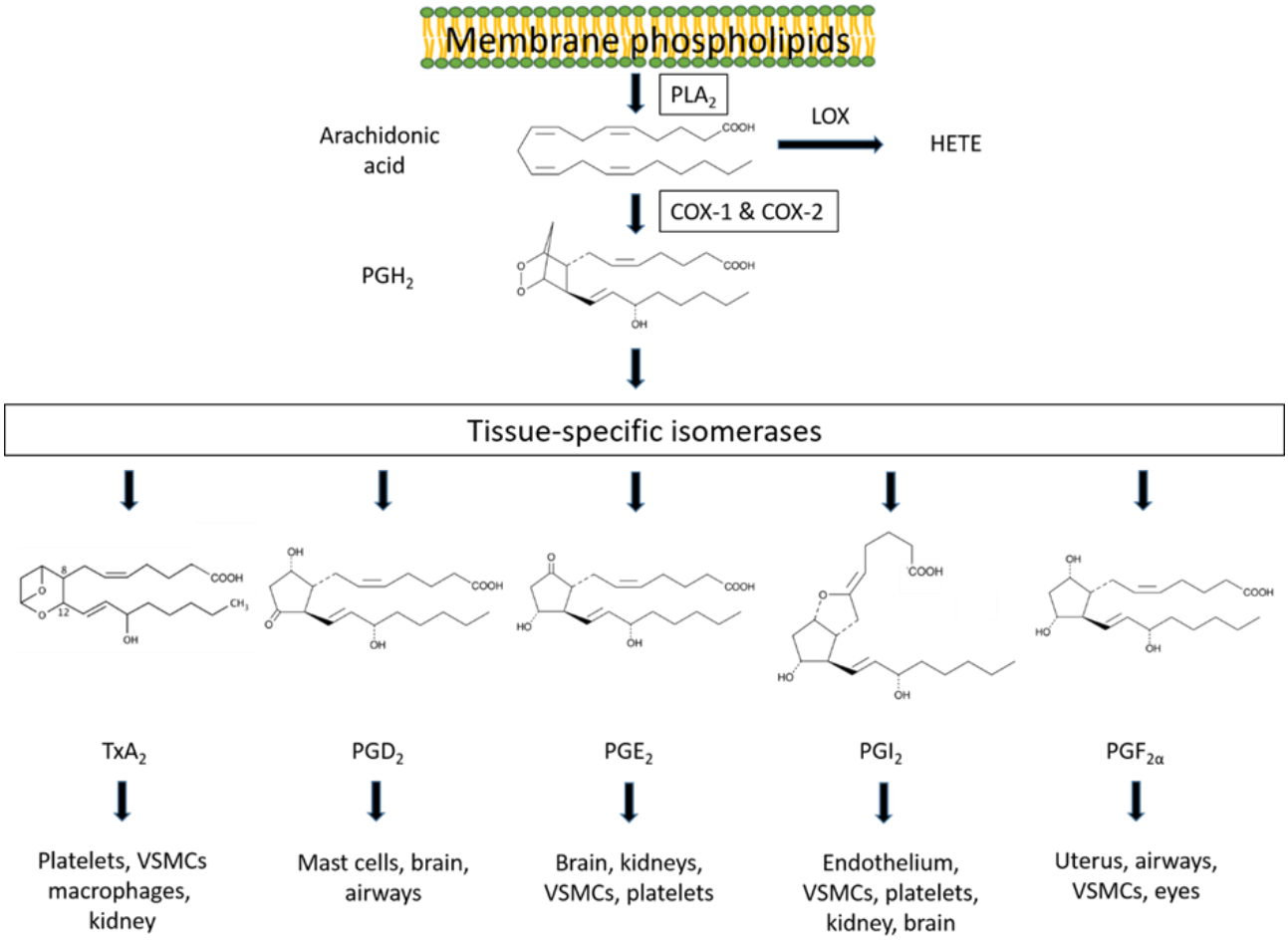

Fig. 1. Synthesis of eicosanoids [8]

PLA_2: phospholipase A_2; COX: cyclooxygenase; PG: prostaglandin; LOX: lipoxygenase; HETE: hydroxyl-eicosatetraenoic acid; VSMCs: vascular smooth muscle cells

The quantity of free AA depends on the cell membrane phospholipid (PL) content, re- or de-acylation of PLs, intracellular calcium ion concentration $[Ca^{2+}]_i$, and the activation of cyclooxygenase-1 or -2 (COX-1, -2) and lipoxygenase (LOX) enzymes. Prostaglandins ($PGF_{2\alpha}$, PGE_2 and PGD_2), thromboxane A_2 (TxA_2) and prostacyclin (PGI_2) are synthesized from cyclooxygenase-derived endoperoxide (PGH_2) by tissue-specific synthetases. Hydroperoxy- and hydroxy-eicosatetraenoic acids are generated by the lipoxygenase pathway [8,9].

Nowadays, the beneficial effects of S1R agonists have been described in various pathological conditions [1], such as sepsis [10], ischemic-reperfusion injury [11], stroke [12] and cardiovascular diseases [13]. Expression of the S1R gene has been shown to decrease inflammatory cytokine production [10] and to play a protective role against the development of diabetic complications [14]. Based on these findings, S1Rs have been implicated in the regulation of not only physiological, but also pathological cellular functions [1,15,16].

Diabetes is a chronic, progressive disease characterized by abnormal carbohydrate, lipid and protein metabolism. These abnormalities lead to the formation of glycation end-products (advanced glycation end products (AGEs)) and accumulation of reactive oxygen species (ROS), resulting in endothelial dysfunction and platelet activation [17,18].

Platelets are small, anuclear cells with a short lifespan (7–9 days) and a specific structure (dense tubular system, various granules, lysosomes, mitochondria and numerous adhesion molecules). This complex structure allows their involvement in haemostasis, cell-cell interaction (with monocytes, endothelial cells and lymphocytes), inflammatory processes, natural and acquired immunity and regulation of microcirculation [19–23]. Bioactive lipid mediators, i.e. eicosanoids (prostaglandins, thromboxane and lipoxygenase products), synthesized by platelets and endothelial cells lining the blood vessel walls, play an important role in these processes [8,24].

Cytokines and eicosanoids synthesized by damaged endothelium and activated platelets are also involved in the development and progression of atherosclerosis as a complication of diabetes mellitus [25–28].

OBJECTIVES

It was previously unknown that platelets possess S1R, and our primary objective was to confirm our hypothesis that platelets express S1R, which may modulate platelet function. We examined the expression of the *Sigmar1* gene in rat platelets by reverse transcription-

polymerase chain reaction and quantitative polymerase chain reaction (RT-qPCR). We also visualized the receptor by immunostaining and confocal laser scanning microscopy.

In several cell types, S1R has been described to affect cell membrane structure and function, as well as intracellular signalling pathways. Therefore, we hypothesized that S1R may also play a role in the physiological function of platelets, which have numerous receptors and intracellular organelles. To confirm this, in our preliminary experiments, we investigated the effects of a known S1R agonist ligand, PRE-084 (2-(4-morpholino)ethyl 1-phenylcyclohexane-1-carboxylate), on platelet AA metabolism and platelet aggregation *in vitro* in healthy rats. Eicosanoid synthesis was determined by radioactive AA-substrate and enzyme-linked immunosorbent assay (ELISA).

It was also important to clarify that subchronic intraperitoneal (i.p.) treatment with a known S1R-agonist, PRE-084, an antagonist, NE-100 (N,N-dipropyl-2-[4-methoxy-3-(2-phenylethoxy)phenyl]-ethylamine monohydrochloride) and a new S1R-ligand, (S)-L1 (S-N-benzyl-6,7-dimethoxy-6,7-dimethoxy-1,2,3,3,3,3, 4-tetrahydro-1-isocinolinolinetamine) [29], can induce *in vivo* changes in AA metabolism in healthy rat platelets and abdominal aorta that can be detected *ex vivo* even in the absence of ligand in the test medium. A preliminary requirement of this series of assays was the determination of blood levels of i.p. administered ligands half an hour after the first administration and before *ex vivo* analysis by liquid chromatography-mass spectrometry (LC-MS).

We hypothesized that S1R ligands may affect not only the quantity of free AA substrate and enzyme activity, but also the mRNA levels of genes encoding S1R and COX derived from megakaryocytes and stored in platelets. To confirm these processes, we determined the effect of S1R ligands on platelet expression of S1R and COX genes.

The role of S1R in inflammation, ischemia-reperfusion injury and oxidative stress has been investigated by several groups. However, the mediating role of platelets and endothelial cells, which play a crucial role in these pathological processes, in the action of S1R has not yet been demonstrated. To study all these, we have established a streptozotocin-induced (STZ-induced) diabetes animal model representative of these pathological processes. Our aim was first to clarify whether STZ-induced diabetes affects laboratory parameters, platelet S1R and cyclooxygenase mRNA levels, platelet and aortic AA metabolism in rats, using radioactive AA substrate and ELISA. We then examined whether treatment with i.p. sub-chronic S1R ligands alters these parameters.

MATERIALS AND METHODS

Animals

Animal experiments were performed under a protocol approved by the Ethical Committee for the Protection of Animals in Research at the University of Szeged, Hungary (Permit No. X./238/2019.). All experiments were carried out in accordance with the Guide for the Care and Use of Laboratory Animals published by the US National Institutes of Health. Male Wistar *(Rattus norvegicus)* rats were used in this study [29–31].

Separation of platelets

Under anaesthesia (Euthasol®/pentobarbital-Na/ 30 mg/kg body weight i.p.), blood was drawn from the abdominal aorta of rats with a thick needle and diluted (1:2) with phosphate buffer (pH 7.4) containing ethylene diamino tetraacetic acid (EDTA, 5.8 mM) and glucose (5.55 mM). Platelets were separated by differential centrifugation [29–31]. After the last centrifugation, the platelets were re-suspended (2.5 x 10^8 platelets/mL) in serum-free Medium 199 tissue culture (Sigma, St. Louis, MO).

Isolation of aorta

Under anaesthesia (Euthasol®/pentobarbital-Na/ 30 mg/kg body weight i.p.), after blood collection, the abdominal aorta of the rat was isolated from the branch of the iliac artery to the diaphragm. At 4°C temperature, the connective tissue was removed from the aorta, which was sliced into 1–2 mm thick rings with care so as not to damage the endothelium. 15 mg wet weight aortic rings per sample were placed in each mL of Medium 199 tissue culture [29,30,32].

Determination of S1R gene expression in non-activated platelets of healthy, untreated rats

Total RNA was isolated from non-activated rat platelet samples with TriFast reagent (VWR International, USA), and then 1 μg RNA from each sample was transcribed to complementary DNA with the Maxima First Strand cDNA Synthesis Kit (Thermo Fisher, USA). For the RT-PCR, previously designed specific oligonucleotide primer pairs were used for the rat S1R gene (*Sigmar1;* NM_030996.1) [33]. For reference, primers for the rat glyceraldehyde 3-phosphate dehydrogenase gene (*Gapdh*; NM_017008.4) were used [34]. The RT-PCR occurred with FIREPol DNA polymerase (Solis BioDyne, Estonia) in a T100 Thermal Cycler (Bio-Rad Laboratories, USA). PCR protocol steps were published in Platelets [31]. The qPCR occurred with a 2x FastStart TaqMan Probe Master mix (Roche, Basel, Switzerland) in a Rotor-Gene 3000 instrument (Qiagen, Hilden, Germany) with inventoried TaqMan Gene

Expression Assays (Life Technologies, USA). qPCR protocol steps were published in Platelets [31]. qPCR data were analysed with Rotor-Gene Real-Time Analysis Software 6.0 (Corbett Research, Australia). In all samples, the expression level of the genes was normalized to the average of endogenous control genes *Gapdh* and β-actin *(Actb)* ($\Delta C_t = C_{tgene} - C_{tcontrol\ genes}$) [31].

S1R visualization by immunostaining and confocal laser scanning microscopy

For the immunostaining of S1R, freshly isolated non-activated rat platelets (4×10^6 platelets/coverslip) were gently seeded on poly-l-lysine coated [35] glass coverslips (1 cm^2, borosilicate, VWR, USA) and incubated for 30 min at room temperature. Platelet samples were fixed with 3% paraformaldehyde for 15 min and permeabilized with 0.5% Triton-X100 in 3% BSA-PBS for 10 min; non-specific binding sites were then blocked with 3% BSA-PBS for 1 h. All steps occurred at room temperature. Samples were incubated over night at 4°C with S1R mouse monoclonal antibody (Sigma Receptor Antibody B-5, sc-137075, Santa Cruz Biotechnology, USA; 2 μg/mL in 3% BSA-PBS). Then samples were washed with PBS and incubated for 1 h at room temperature with goat anti-mouse secondary antibody Alexa 555 (A21424; Invitrogen, Thermo Fisher, USA; 4 μg/mL in PBS) and Falloidin-CF488A (00042, Biotium, USA; 1:100 dilutions in PBS) to stain F-actin with alpha-tubulin monoclonal antibody (T6199, Sigma, USA; 1 μg/mL in 3% BSAPBS) or with Alexa 488 conjugated wheat germ agglutinin (WGA), lectin (W11261, Invitrogen; 5 μg/mL) to stain N-acetyl-D-glucosamine and sialic acid components. Samples were washed with PBS after each step and mounted using Fluoromount-G (Southern Biotech, USA). Staining was visualized with a confocal laser scanning microscope (Leica SP5, Leica Microsystems GmbH, Germany). To prove the absence of non-specific staining, we added a negative control group stained only with the secondary antibody Alexa 555 [31].

Binding pose determination of PRE-084 and *(S)*-L1 S1R ligands

The PRE-084 and *(S)*-L1 were docked to the target, which is C-chain from the X-ray structure of the S1R (PDB ID: 6DK1), using the Glide program from the Schrödinger package [36]. Prior to docking, the necessary fields were calculated on a uniform, 1 Å-spaced grid inside a cube with ~32 Å –long edges. The grid centres were located at the centre of the ligands from the X-ray structures used. Compounds were prepared for docking with Ligprep [36] and used in an extra precision (XP) docking protocol [36] with the OPLS3e force field [37] for parameterization [29].

Establishment of diabetic rat group

Diabetes mellitus was induced in eleven-week-old, male Wistar rats with a single i.p. injection of 65 mg/Bwkg STZ (Sigma, St. Louis, MO, USA) that was dissolved in 50 mM citrate buffer. After STZ injection, the drinking water of animals was changed for 10% (w/v) sucrose solution for 24 h [38]. Rats were considered diabetic if the fasting (12 h) peripheral blood glucose concentration was higher than 20 mM 72 h after the injection of STZ (initial serum glucose level). Serum glucose level was monitored by Dcont equipment and Ideal test strips (77 Elektronika Ltd., Budapest, Hungary).

Experimental animal groups to study the *in vivo* effects of S1R ligands

The subchronic, *in vivo* effects of S1R ligands were investigated in a total of 81 male Wistar rats (Rattus norvegicus) (Fig. 2) [30].

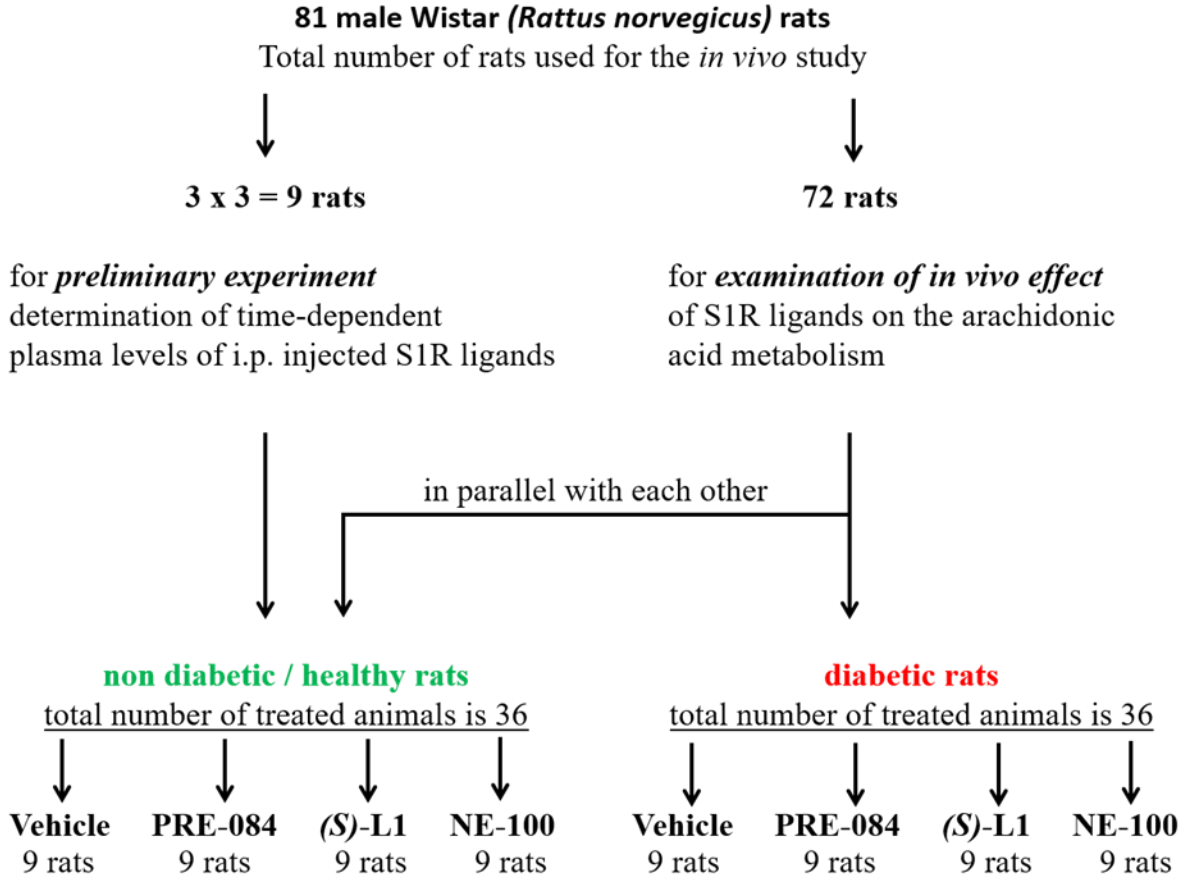

Fig. 2. Experimental animal groups to study the *in vivo* effects of S1R ligands

After one week of acclimatization to the environment and hand-holding, they were divided into two groups. In our preliminary experiment, nine animals (three animals/group) were used for time-dependent testing of the blood levels of the S1R ligands (PRE-084, *(S)*-L1 and NE-100) after a single i.p. injection of 3 mg/kg body weight. The remaining 72 rats were used to

investigate the effects of the S1R ligands on platelets *in vivo/ex vivo* and aortic arachidonic acid metabolism. The animals were divided into two groups. One group of 36 rats was the healthy population, while the other group consisted of diabetic animals treated with STZ (see the diabetic animal model section of the manuscript). The healthy and diabetic animal populations, each consisting of 36 rats, were divided into subgroups of nine rats. One group of rats was treated with vehicle (isotonic saline), and the other three groups with one of the S1R ligands (3 mg/kg bw, i.p.). Therefore, the generated subgroups were as follows: (1) the control/vehicle-treated, (2) the PRE-084-treated (MedChem Express USA), (3) the *(S)*-L1-treated (a novel high affinity S1R ligand screened in silico from the in-house compound library of Institute of Pharmaceutical Chemistry, University of Szeged) [39], and (4) the NE-100-treated (Tocris Bioscience, Bristol, UK) (Fig. 2). Before the *ex vivo* experiment, the physical and laboratory parameters of the animals were tested [29,30].

Determination of serum S1R ligands levels

Serum ligand (PRE-084, *(S)*-L1 and NE-100) concentrations in sub-chronic, *in vivo* S1R ligand-treated rats were determined by liquid chromatography-mass spectrometry/mass spectrometry (LC-MS/MS) (A detailed description of the method can be found in Váczi et al. [29]).

Determination of S1R and cyclooxygenase (COX) gene expression in the platelets of healthy and diabetic rats

The gene expression of S1R (*Sigmar1*), COX-1 (prostaglandin G/H synthase 1, *Ptgs1*) and COX-2 (prostaglandin G/H synthase 2, *Ptgs2)* enzymes was determined in platelets from animals treated *in vivo* with S1R ligands. Rat platelet samples were homogenized in TRI Reagent (Sigma-Aldrich, USA), and then RNA from each sample was transcribed to complementary DNA using a High Capacity cDNA Reverse Transcription Kit (Applied Biosystems, USA) according to the manufacturer's protocol based on random priming. The RT-qPCR was performed with two technical parallels from one biological simple (total of four reactions per group) using TaqMan Gene Expression Master Mix (Life Technologies, USA) in a Bio-Red C1000 Touch Thermal Cycler (Bio-Rad Laboratories, USA). Inventoried TaqMan Gene Expression Assays (Life Technologies, USA) were the following: *Sigmar1*-Rn00578590_m1; *Ptgs1*-Rn00566881_m1; *Ptgs2*-Rn01483828_m1; *Gapdh*-Rn01749022_g1. After heat activation at 95°C for 3 min, the cycling conditions were the following: denaturation for 30 s at 95°C, amplification for 30 s at 60°C (40 cycles). qPCR data were analysed with Bio-Rad CFX Maestro software (Bio-Rad Laboratories, USA). In all the

samples, the transcript level of a gene was normalized to an endogenous control gene (*Gapdh*, $\Delta Ct = Ct_{gene} - Ct_{Gapdh}$). Then $\Delta\Delta Ct$ was calculated in comparison with the relative expression of the target genes in the vehicle-treated control groups. Fold changes were calculated using the $2^{-\Delta\Delta Ct}$ formula [29,30].

Analysis of eicosanoid synthesis

AA metabolism studies using radioactive substrate

To investigate the effect of PRE-084 on platelet AA metabolism *in vitro*, platelets (2.5×10^8 platelets/ml Medium 199/sample) were pre-incubated with PRE-084 (0; 0.5; 1; 1; 2; 4 μM) ligand at 37°C for 3 min [31]. When *ex vivo* eicosanoid synthesis was tested following sub-chronic *in vivo* S1R ligand treatment, platelets (2.5×10^8 platelets/mL Medium 199/sample) were pre-incubated at 37°C for 3 min and aortic rings (15 mg wet wt/mL Medium 199/sample) for 10 min [29,30]. In all cases, the radioactive enzyme reaction was started with the addition of the tracer substrate (1-^{14}C-arachidonic acid (3.7 kBq, 0.172 nM/sample; American Radiolabeled Chemicals, Inc., St. Louis, MO, USA) to the incubation mixture. The enzyme reaction was stopped by bringing the pH to 3 with formic acid after 13 min of incubation in the case of the platelet samples and after 30 min of incubation in the case of the aortic samples. The subsequent steps of the study, both *in vitro* and *in vivo/ex vivo*, were exactly the same. The samples were extracted with ethyl acetate, and the organic phases were evaporated. The residues were reconstituted in ethyl acetate and quantitatively applied to silica gel G thin-layer plates (Kieselgel G 60/DC-Fertigplatten, Merck, Art. 5721). The plates were developed to a distance of 16 cm in the organic phase of ethyl acetate:acetic acid:2,2,4-trimethylpentane:water (110:20:30:100) using overpressure thin-layer chromatography (Chrompress 25, Labor MIM, Hungary) [32,40–42]. A semi-quantitative analysis of labelled AA metabolites was performed with a BIOSCAN AR-2000 Imaging Scanner (Eckert & Ziegler Radiopharma, Berlin, Germany) using Win-Scan 2D Imaging Software. The radio-labelled products of arachidonic acid were identified with unlabelled authentic standards [43].

Analysis of eicosanoid synthesis by ELISA

The course of this procedure is the same as that of the examination of radioactive AA metabolism (see above), but, in this case, the radioactive-labelled substrate is not added to the incubation mixture. After incubation, the incubation mixture, which contained either platelets or aortic rings, was placed at -80°C and stored at this temperature until the assay was performed. Before the ELISA test was conducted, the samples were lyophilized and the lyophilizates were re-suspended in the 310 μL 0.9% NaCl solution as the original incubation

medium. The prepared samples were centrifuged at 3000 rpm, for 10 min to remove cell debris. Subsequently, the quantity of COX-1 (sensitivity: 0.285 ng/mL; assay range: 0.3–60 ng/mL) and COX-2 (sensitivity: 0.446 ng/mL; assay range: 0.5–150 ng/mL), or TxB_2 (sensitivity: 5.48 ng/L; assay range: 5–1800 ng/L) was determined in the rat platelets and aorta with ELISA kits (Shanghai Sunred Biological Technology Co. Ltd. PRC) in compliance with the protocols attached to the kits. The optical absorbance of the samples was measured at 450 nm using a STAT FAX 2100 ELISA plate reader (Awareness Technology, Inc. Palm City, FL, USA). Based on the calibration curves, the respective concentrations of the metabolites and enzymes under examination were determined using the SPSS 22.0 software [29–31].

Platelet aggregometry

Preparation of blood samples for aggregometry

Whole blood was collected from the abdominal aorta of rats anaesthetized by pentobarbital (Euthasol®, 30 mg/kg body weight i.p.) in a plastic tube containing 15 μg/mL hirudin (Roche Ltd. Budapest, Hungary). The aggregometry was carried out within 90 min after the collection of blood [44–47]. The platelet count was determined and standardized. All of the cuvettes for aggregometry contained the same quantity of platelets (2.5–3.5 × 10^8 platelets/mL). The platelet count was also measured after the aggregation to detect potential thrombocytolysis. The total volume of the test cuvette was 620 μL. According to the original measurement protocol for the device, the solution contains the following: 300 μL whole blood, 300 μL 0.9% NaCl solution, and 20 μL inducer. To investigate the effects of the S1R agonist, we slightly modified this protocol. We used the aggregometer in a semi-automatic mode. The basic principle was the following: with every addition of 20 μL S1R agonist PRE-084 (diluted in physiological saline solution), we reduced the quantity of 0.9% NaCl solution by 20 μL, thus keeping the final volume of the solution constant (620 μL). The inducers in the 620 μL solution were the following: ADP (6.5 μM) or AA (0.5 mM) [47].

Multiple-electrode aggregometry (MEA)

The Multiplate® analyser provides a disposable test cuvette featuring a duplicate sensor (Roche Ltd. Budapest, Hungary). The electric impedance (Ω) occurring between the electrodes positively correlates with the rate of platelet aggregation. The device uses arbitrary units (AU; 1 AU ≈ 8 Ω). The aggregation curve is the quantitative display of the reaction, and it represents the rate of aggregation expressed as AU plotted against time. The curve is characterized by the following parameters: area under the curve (AUC) in units (U), providing

the most precise assessment of the whole reaction; speed in units (AU/min), representing the slope of the curve (speed of aggregation or SA), which supplies information about the initial kinetics of the reaction (primary aggregation); and the peak of the curve expressed as AU, showing the maximum aggregation (MA) during the whole reaction [45–47].

Treatment of blood samples and aggregometry

In our current study, we used two inducers, AA (ASPItest) and ADP (ADPItest), purchased from Roche Ltd. (Switzerland). Before use, the lyophilized inducers were carefully dissolved in 1 mL ion-free water. After 10 minutes at room temperature, the solution was ready to be used. At first, the effect of the inducers was assessed. We measured 300 μL whole blood and 300 μL 0.9% NaCl solution into the test cuvette. After 3 min of incubation outside the aggregometer, the cuvette was attached to the device, and another 3 min of incubation was performed. Then the aggregation reaction was initiated by administering 20 μL of AA (0.5 mM) or ADP (6.5 μM). The measurement was performed with both inducers in each sample. The S1R agonist PRE-084 was applied in different concentrations (1, 2, 4, 8 μM). In this experimental setup, 20 μL PRE-084 was added to 300 μL blood and 280 μL saline. After 3 min of incubation outside the aggregometer, the cuvette was attached to the device and another 3 min of incubation was performed. Then the aggregation reaction was initiated by administering 20 μL of AA (0.5 mM) or ADP (6.5 μM). The measurement was carried out with both inducers on every blood sample [47].

Statistical analysis

The normality of the results was checked with the Kolmogorov–Smirnov test, as the variances were different with Levene's test. The physical and laboratory parameters of the animals, the eicosanoid synthesis results of ELISA and the labelled AA substrate were assessed by one-way analysis of variance (ANOVA) or Welch's ANOVA followed by the Bonferroni, Tukey or Dunnett's T3 post hoc test. The results of the RT-qPCR tests were assessed by one-way ANOVA followed by Dunnett's post hoc test. The exact statistics for the data are shown below the figures. A difference at a level of $p < 0.05$ was considered statistically significant. The results are expressed as means ± S.D. The statistical analysis was performed by SPSS version 22.0 (IBM Corp. Released 2013. IBM SPSS Statistics for Windows, Version 22.0. Armonk, NY).

RESULTS

EXPRESSION OF S1R IN NON-ACTIVATED RAT PLATELETS

Platelet morphology was also confirmed with immunocytochemistry for alpha-tubulin in addition to F-actin and lectin staining (Fig. 3). All three stainings of the rat platelets show the structure of the platelets well and fully mark the platelet space (Figs. 3 and 4) [31]. In the non-activated rat platelet samples, the *Sigmar1* gene was expressed as detected by RT-PCR (Fig. 4A). The expression of the housekeeping gene *Gapdh* was also visible. The expression of the *Sigmar1* gene in the non-activated rat platelets was also detected with qPCR (17.3 ± 0.22) and shown as relative expression normalized to the *Gapdh* and *Actb* control genes (Fig. 4B) [31].

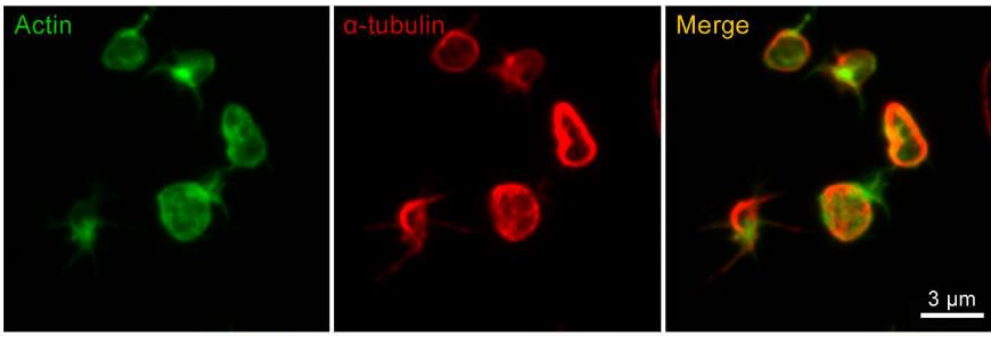

Fig. 3. Morphology of non-stimulated rat platelets

The structure of the platelets was characterized by phalloidin-A488 staining for F-actin and immunostaining for α-tubulin [31]. Scale bar: 3 µm.

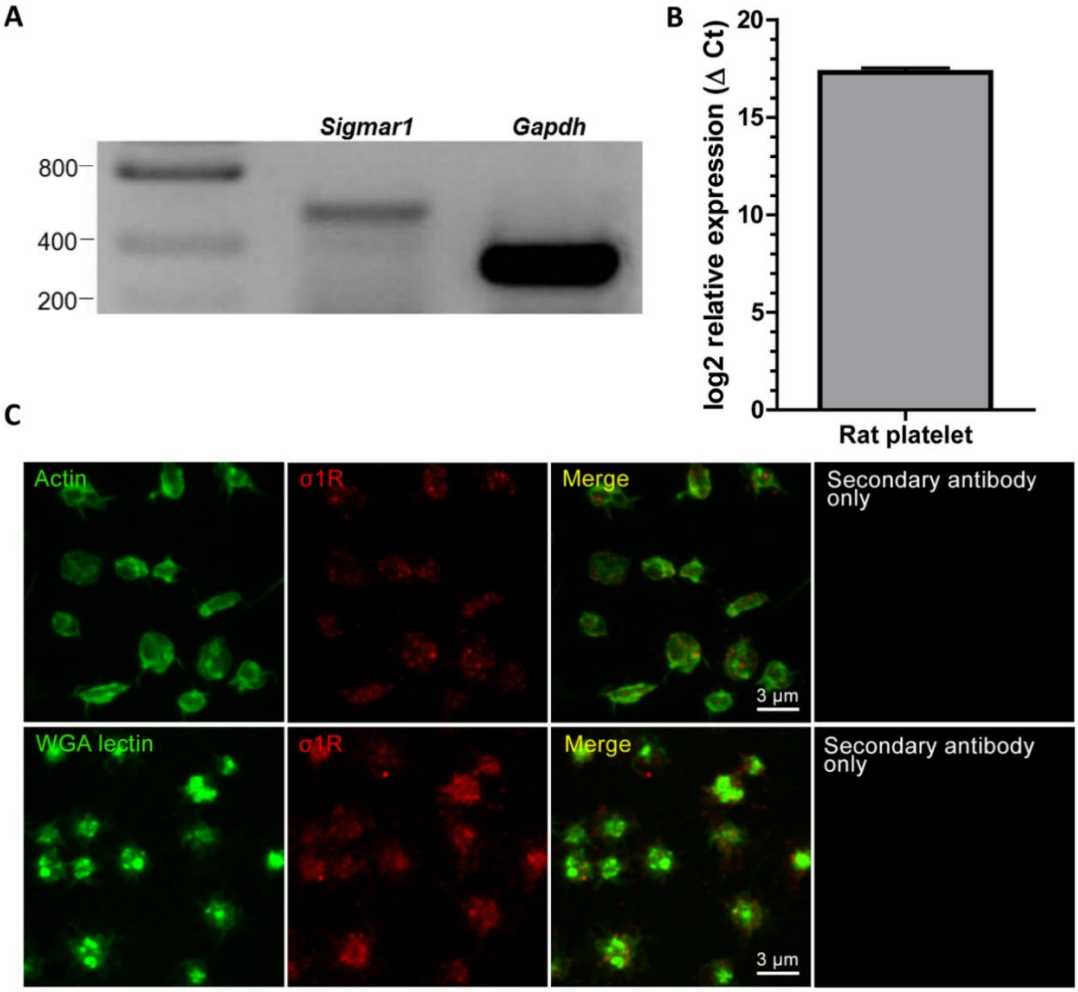

Fig. 4. Expression of Sigma-1 receptor in non-stimulated rat platelet samples [31]

(A) S1R mRNA expression is shown in rat platelets. The predicted PCR product length was 512 bps. The *Gapdh* gene was used as a reference with a predicted product length of 356 bps. Fragments were visualized on 2% agarose gel.

(B) Relative gene expression of S1R in rat platelet samples normalized to endogenous control genes *Gapdh* and *Actb* measured by qPCR. Mean ± SD, n = 3.

(C) Confocal microscopy images of S1R immunostaining in rat platelets. Green: F-actin (upper panels) or wheat germ agglutinin (WGA) lectin staining (lower panels), red: S1R. Scale bar: 3 µm. Negative control group: secondary antibody only.

S1R were also present at the protein level in non-activated rat platelets: the punctate staining pattern was co-localized with the F-actin structure or with the wheat germ agglutinin lectin staining of rat platelets as visualized by confocal microscopy. We did not detect non-specific binding of secondary antibody labelled with Alexa-555 (Fig. 4C) [31].

After detecting the presence of S1R on rat platelets, we investigated the *in vitro* effect of PRE-084, already known as an S1R agonist, on non-activated rat platelets.

IN VITRO EFFECT OF PRE-084 ON NON-ACTIVATED RAT PLATELETS

In vitro effect of PRE-084 on the AA metabolism of rat platelets

Analysis of eicosanoid synthesis using radioactive arachidonic acid

The *in vitro* AA metabolism of non-activated rat platelets was enhanced by all concentrations of PRE-084 that we tested, via both the COX (Fig. 5A) and LOX (Fig. 5B) pathways [31].

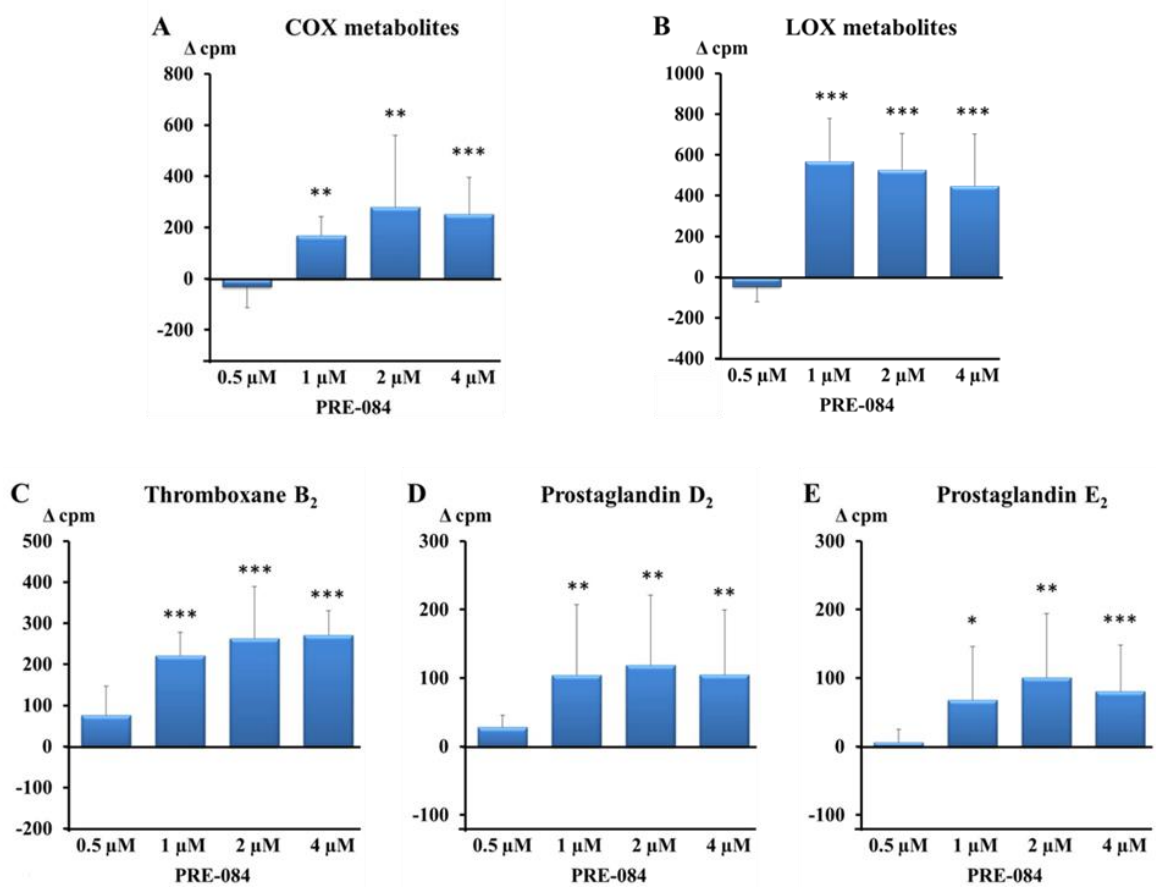

Fig. 5. *In vitro* study of the effect of PRE-084 on AA metabolism of non-activated rat platelets using a radioactive AA substrate

In vitro effect of PRE-084 on the eicosanoids that were synthesized through the cyclooxygenase (COX, Fig. 5A) and lipoxygenase (LOX, Fig. 5B) pathways from the radiolabelled AA in resting rat platelets. COX: total quantity of cyclooxygenase metabolites (sum of thromboxane B_2/TxB_2 (Fig. 5C), prostaglandin D_2/PGD_2 (Fig. 5D), prostaglandin E_2/PGE_2 (Fig. 5E), 6-keto prostaglandin $F_{1\alpha}$/6-k$PGF_{1\alpha}$, prostaglandin $F_{2\alpha}$ /$PGF_{2\alpha}$, and 12-L-hydroxy-5,8,10-heptadecatrienoic acid/12-HHT); LOX: total quantity of lipoxygenase metabolites; PRE-084: 2-(4-morpholino)ethyl-1-phenylcyclohexane-1-carboxylate. Data are mean ± (SD) for nine animals in cpm (count per minute). ANOVA, Tukey test, $^{*}p < 0.05$, $^{**}p < 0.03$; $^{***}p < 0.01$; PRE-084 *in vitro* pre-treated vs. control sample.

The total quantity of metabolites formed by the COX pathway and the synthesis of TxB_2 (Fig. 5C), PGD_2 (Fig. 5D) and PGE_2 (Fig. 5E) were enhanced most significantly by the 2 µM concentration of PRE-084. These effects were not further enhanced by increasing the concentration of PRE-084. The dose response curves for PRE-084 were sigmoidal for all COX products mentioned above [31].

Analysis of eicosanoid synthesis by ELISA

The quantitative analysis of the *in vitro* effect of PRE-084 on the eicosanoid synthesis of non-activated platelets was performed by ELISA. The 2 μM PRE-084, which induced a significant increase in eicosanoid synthesis when the radioactive substrate was applied, raised the concentrations of both COX-1 (48.4 ± 8.3 ng/ml vs. 11.3 ± 2.5 ng/ml) (Fig. 6A) and TxB_2 (0.528 ± 0.16 ng/ml vs. 0.194 ± 0.038) (Fig. 6B) compared to the control sample [31].

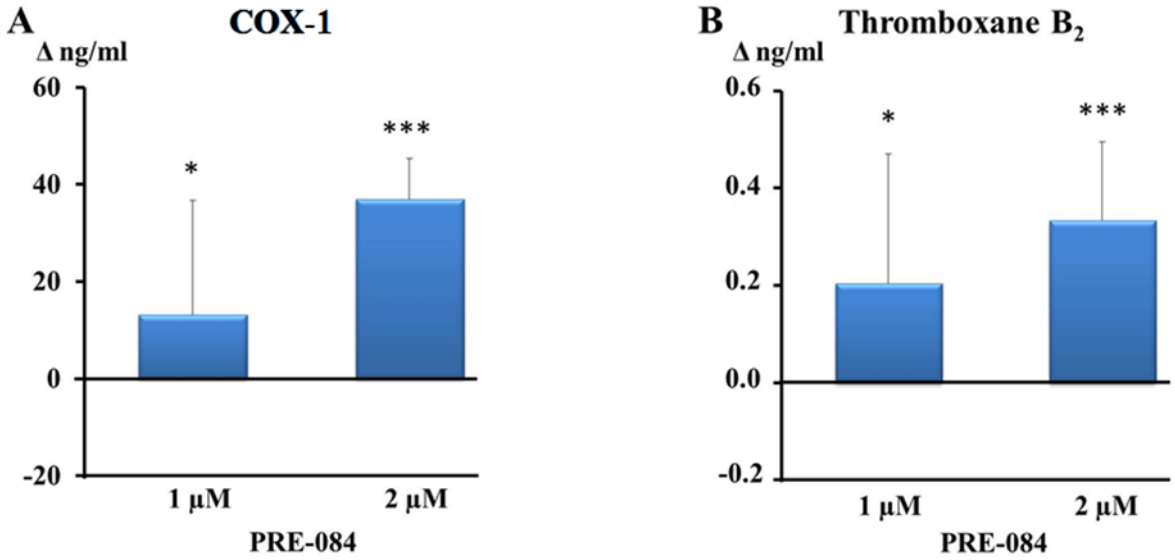

Fig. 6. *In vitro* analysis of the effect of PRE-084 on AA metabolism of non-activated rat platelets by ELISA

COX-1: type 1 of cyclooxygenase; TxB_2: thromboxane B_2. Data are mean ± (SD) for six animals. ANOVA, Tukey test, $^{*}p < 0.05$, $^{**}p < 0.03$; $^{***}p < 0.01$, PRE-084 *in vitro* pre-treated sample compared to control. ELISA: enzyme-linked immunosorbent assay; PRE-084: 2-(4-morpholino) ethyl-1-phenylcyclohexane-1-carboxylate, S1R agonist

Effect of PRE-084 on healthy rat platelet aggregation

All of the characteristic parameters of the aggregation curves (AUC, MA and SA) were elevated by PRE-084 for both AA- and ADP-induced platelet aggregation compared to the control samples. The 2 μM concentration of PRE-084 was the smallest effective concentration. No augmentation of platelet aggregation was observed when the agonist concentration was further increased, suggesting a concentration-response curve with a plateau phase. The greatest effect of PRE-084 was observed on the velocity of the AA-induced aggregation compared to control samples. We detected no significant difference between the AA- or ADP-induced platelet aggregation for the same agonist concentration (Table 1) [31].

Arachidonic acid (AA, 0.5 mM)-induced aggregation					
	Control	**PRE-084**			
		1 μM	**2 μM**	**4 μM**	**8 μM**
AUC (U)	44.9±7.2	48.4±8.5	57.1±13.8**	57.8±12.0***	60.5±11.3***
MA (AU)	71.1±11.7	77.0±13.7	88.0±20.4**	88.6±16.5***	91.3±16.1***
SA (AU/min)	13.8±2.7	15.1±3.4	19.4±4.9**	20.8±5.6***	21.8±4.6***
Adenosine diphosphate (ADP, 6.5 μM)-induced aggregation					
	Control	**PRE-084**			
		1 μM	**2 μM**	**4 μM**	**8 μM**
AUC (U)	48.1±8.0	52.8±5.9	57.9±9.5*	58.9±11.6**	60.8±7.9**
MA (AU)	70.3±9.2	77.4±6.9	84.6±11.6*	86.3±13.8**	87.9±9.2**
SA (AU/min)	16.3±4.0	17.5±2.8	20.5±5.1*	20.7±5.4*	21.8±3.8**

Table 1. *In vitro* effect of S1R agonist PRE-084 on the platelet aggregation [31]

Data are mean ± (SD) of nine animals. ANOVA, Tukey test, $^{*}p < 0.05$, $^{**}p < 0.03$; $^{***}p < 0.01$; PRE-084 pre-treated vs. control sample; AA: arachidonic acid; ADP: adenosine diphosphate; AU: arbitrary aggregation unit; AUC: area under the curve; AU/min: arbitrary aggregation unit / minute; MA: maximal aggregation; PRE-084: 2-(4-morpholino)ethyl-1-phenylcyclohexane-1-carboxylate, sigma-1 receptor agonist; SA: speed of aggregation; U: unit [31].

Our preliminary experiments have demonstrated the platelet function enhancing effect of PRE-

084 in rats. We also wanted to extend our studies to other S1R ligands. We wanted to study the effect of the S1R antagonist NE-100. In addition, we wished to study the effect of a new high-affinity ligand, *(S)*-L1. The latter was selected from the in-house compound library of the Institute of Pharmaceutical Chemistry, University of Szeged, by in silico screening in collaboration with Dvorácskó et al.[39].

MOLECULAR MODELLING OF THE DOCKING OF THE LIGANDS TO S1R

The chemical structures of PRE-084, NE-100 and *(S)*-L1 are shown in Figure 7A. All ligands fit Glennon's early pharmacophore model [48]. It contains the following structural elements: a basic amine site, which is required to form an electrostatic bond with Glu172 of the receptor, and two distinct hydrophobic groups surrounding it. The hydrophobic moieties are mostly aromatic and/or rigid heterocyclic sites. The binding modes of these ligands are compared in Figure 7B. The binding pose of NE-100 was obtained from the X-ray structure of the ligand-bound S1R (PDB ID: 6DK0). The binding poses of the other two ligands were obtained by

Glide XP docking to the apo receptor from the C-chain of the PDB 6DK1 structure. According to Schmidt and co-workers [49], the main difference between agonist and antagonist binding is the presence of ligand interaction with the C-terminal helix shown in the foreground of Figure 7B [29].

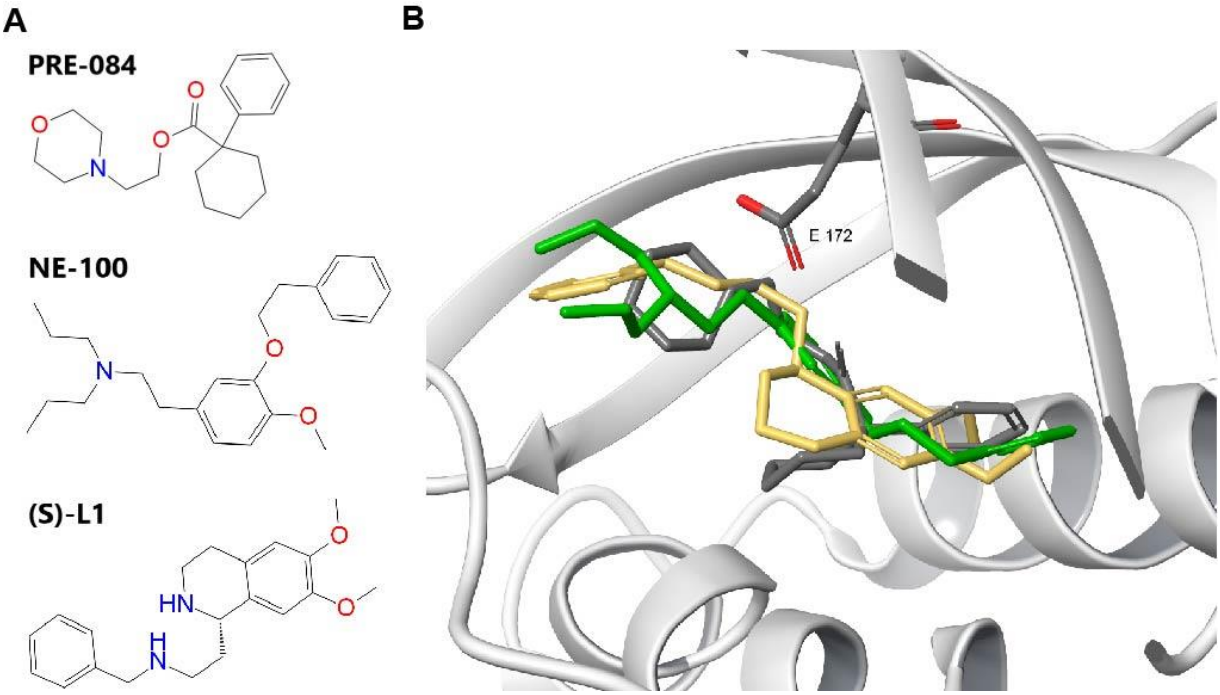

Fig. 7. (**A**) **Chemical structure of sigma-1 receptor ligands** (PRE-084, NE-100, *(S)*-L1). (**B**) **Binding pose** of agonist PRE-084 (grey), antagonist NE-100 (green) and *(S)*-L1 (yellow) [29]

The binding pose of NE-100 was extracted from the X-ray structure of the ligand bound S1R (PDB ID: 6DK0). The binding pose of the other two ligands was obtained with Glide XP docking to the apo receptor extracted from the C chain of PDB structure 6DK1. To superimpose the binding pockets of 6DK0 and 6DK1 we used the backbone atoms of residues 170-176 and 197-217.

The cyclohexane ring of PRE-084 is the only part that is able to interact with this helix [49]. The *(S)*-L1 and the S1R antagonist NE-100 have very similar binding positions [29].

Our *in vitro* preliminary experiments allowed the demonstration of acute effects of PRE-084 on rat platelets. The study of the *in vivo*, sub-chronic effects of S1R ligands required intraperitoneal ligand administration and determination of the serum levels of each compound.

CONCENTRATION OF S1R LIGANDS IN PLASMA

In the preliminary experiments

Prior to the *in vivo* administration of the S1R ligands, we monitored the kinetic changes in the plasma levels of PRE-084, *(S)*-L1 and NE-100 administered intraperitoneally as a single dose in the male rats (Fig. 8) [29].

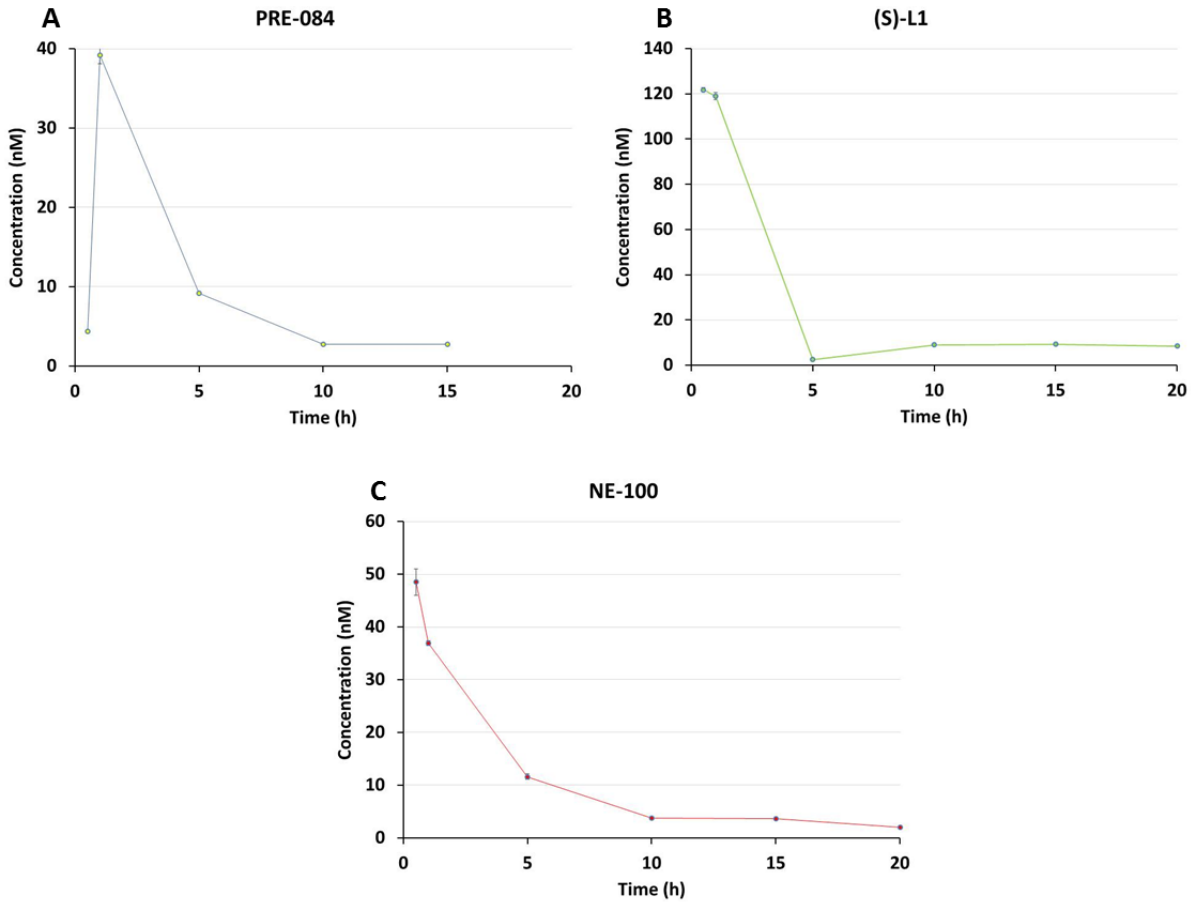

Fig. 8. The mean plasma concentration-time dependence of PRE-084 (A), *(S)*-L1 (B) and NE-100 (C) in rat plasma after intraperitoneal administration (single dose, 3 mg/Body weight kg/mL) (n = 3 each) [29]

A significant elevation in plasma levels was detected 1 h after the administration of PRE-084 and 30 min after the administration of *(S)*-L1 and NE-100. The ligand concentration rapidly decreased, and the quantity of S1R ligands was insignificant or undetectable 20 h after the injection (Fig. 8) [29,30].

In the terminal phase of the *in vivo* experiments

Plasma concentrations of the S1R ligands were determined in all of the healthy and diabetic rats 20 h after the last ligand injection immediately before the *ex vivo* studies (Table 2).

Analyte	**Concentration (nM)**	
	Healthy/Non-diabetic rats	**Diabetic rats**
PRE-084	< LOQ	< LOQ
***(S)*-L1**	5.64 ± 0.32	10.99 ± 1.06
NE-100	< LOD	5.31 ± 3.14

Table 2. Concentration of the S1R ligands in rat plasma. Samples were taken 20 h after the last dose (3 mg/Bwkg/day for seven days) [29,30]

Data is shown as mean ± SD; n = 9 rats/group; LOQ: limit of quantification; LOD: limit of detection.

The plasma concentrations of the S1R ligands were below the limit of detection or quantification 20 h after the last dose (Table 2). PRE-084 was eliminated from the circulation the fastest of all the S1R ligands we tested, while *(S)*-L1 was eliminated the most slowly [29,30].

LABORATORY RESULTS OF HEALTHY AND DIABETIC RATS TREATED *IN VIVO*

At the end of the *in vivo* study (terminal phase), the levels of total cholesterol, alanine aminotransferase (ALT) and blood urea nitrogen (BUN) were determined from the pooled plasma samples (Fig. 9) [29,30].

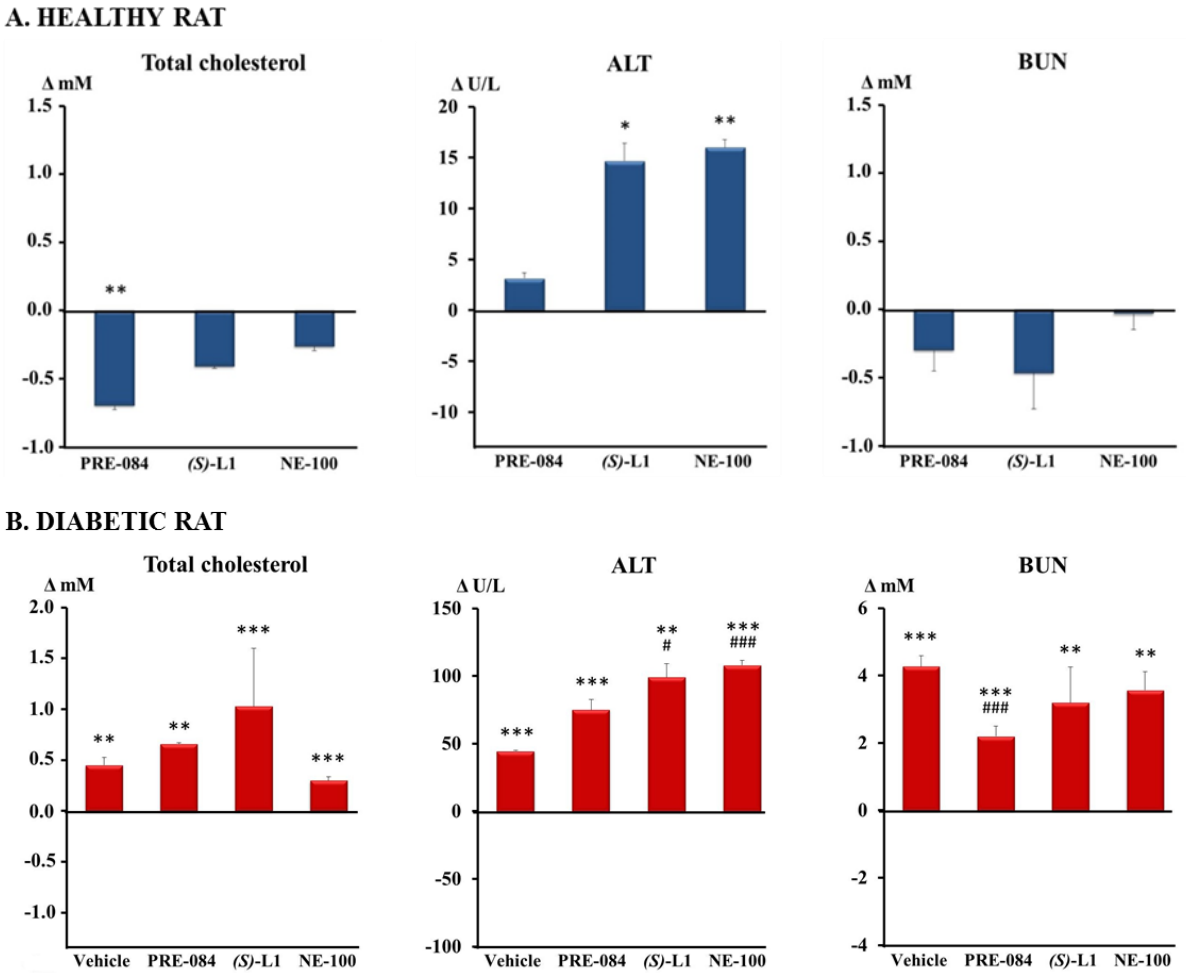

Fig. 9. Laboratory parameters of healthy and diabetic rats at the end (terminal phase) of the *in vivo* study

Fig. 9, **row A** shows the plasma serum total cholesterol, alanine aminotransferase (ALT) and blood urea nitrogen (BUN) levels ***in healthy*** PRE-084-, *(S)*-L1- or NE-100-treated ***rats*** as compared to the vehicle-treated, healthy ones.

Fig. 9, **row B** shows the levels of the same laboratory parameters as row A, but ***in diabetic*** vehicle-, PRE-084-, *(S)*-L1- or NE-100-treated rats compared to vehicle-treated healthy and diabetic rats.
In both rows in the figure, the zero line shows the average plasma concentrations of healthy rats treated with vehicle, while the bars in the figure show the average plasma concentrations of healthy (Fig. 9A) or diabetic (Fig. 9B) treatment groups; n = 3 samples, pooled from nine rats per group; Welch ANOVA, Dunnett's T3 test,

$^{**}p<0.\ 03$, $^{***}p<0.01$ compared to the vehicle-treated healthy rat group; $^{\#}p<0.05$, $^{\#\#\#}p<0.01$ compared to the vehicle-treated diabetic rat group [29,30].

In healthy rats, sub-chronic *in vivo* treatment with PRE-084 induced a decrease in serum total cholesterol levels, whereas *(S)*-L1 and NE-100 induced an increase in serum ALT. However, blood urea nitrogen (BUN) levels were not altered by any of the S1R ligands we tested compared to the vehicle-treated healthy animals (Fig. 9A). The serum total cholesterol, ALT and BUN levels in the STZ-induced diabetic animals treated with vehicle were higher (cholesterol by 21%; ALT by 120%; BUN by 63%) than those of the healthy rats studied in parallel with the present experiment. PRE-084 and NE-100 significantly elevated serum cholesterol and BUN in the diabetic rats compared to the vehicle-treated, healthy animals. In the diabetic rats, all three S1R ligands further enhanced the STZ-induced increase in plasma ALT levels compared to the vehicle-treated, healthy animals. None of the S1R ligands tested significantly altered the rise in serum cholesterol levels induced by STZ treatment. *(S)*-L1 and NE- 100 further enhanced the growth in ALT levels observed in the vehicle-treated, diabetic rats. The smallest growth in ALT was detected when PRE-084 was used. An STZ-induced rise in BUN levels was only attenuated by PRE-084 (Fig. 9B) [29,30].

EFFECTS OF SUB-CHRONIC, *IN VIVO* ADMINISTRATION OF S1R LIGANDS

Ex vivo effects of S1R ligands on platelets

Ex vivo effects of S1R ligands on the eicosanoid synthesis of platelets

Analysis of eicosanoid synthesis using radioactive arachidonic acid

In healthy rat platelets, the total quantity of radioactive COX metabolites (the sum of 6-keto prostaglandin $F_{1\alpha}$/6-k-$PGF_{1\alpha}$; prostaglandin $F_{2\alpha}$/$PGF_{2\alpha}$; prostaglandin E_2/PGE_2; prostaglandin D_2/PGD_2; thromboxane B_2/TxB_2, which is a stable metabolite of TxA_2; and 12-L-hydroxy-5,8,10-heptadecatrienoic acid/12-HHT) was significantly reduced by PRE-084 and *(S)*-L1, while it was elevated by NE-100 (Fig. 10A) [29]. However, the total quantity of radioactive LOX metabolites was raised by PRE-084 and *(S)*-L1, but was lowered by NE-100, thus indicating an opposite effect on the total quantity of radioactive COX and LOX metabolites (Fig. 10A) [29].

In the platelets, one month after the development of *STZ-induced diabetes*, neither the total quantity of the COX metabolites nor that of the LOX metabolites was altered compared to healthy rats. In the diabetic rat platelets, the total quantity of the COX metabolites was significantly elevated by NE-100 compared to the vehicle-treated, healthy rat platelets (Fig. 10B) [30].

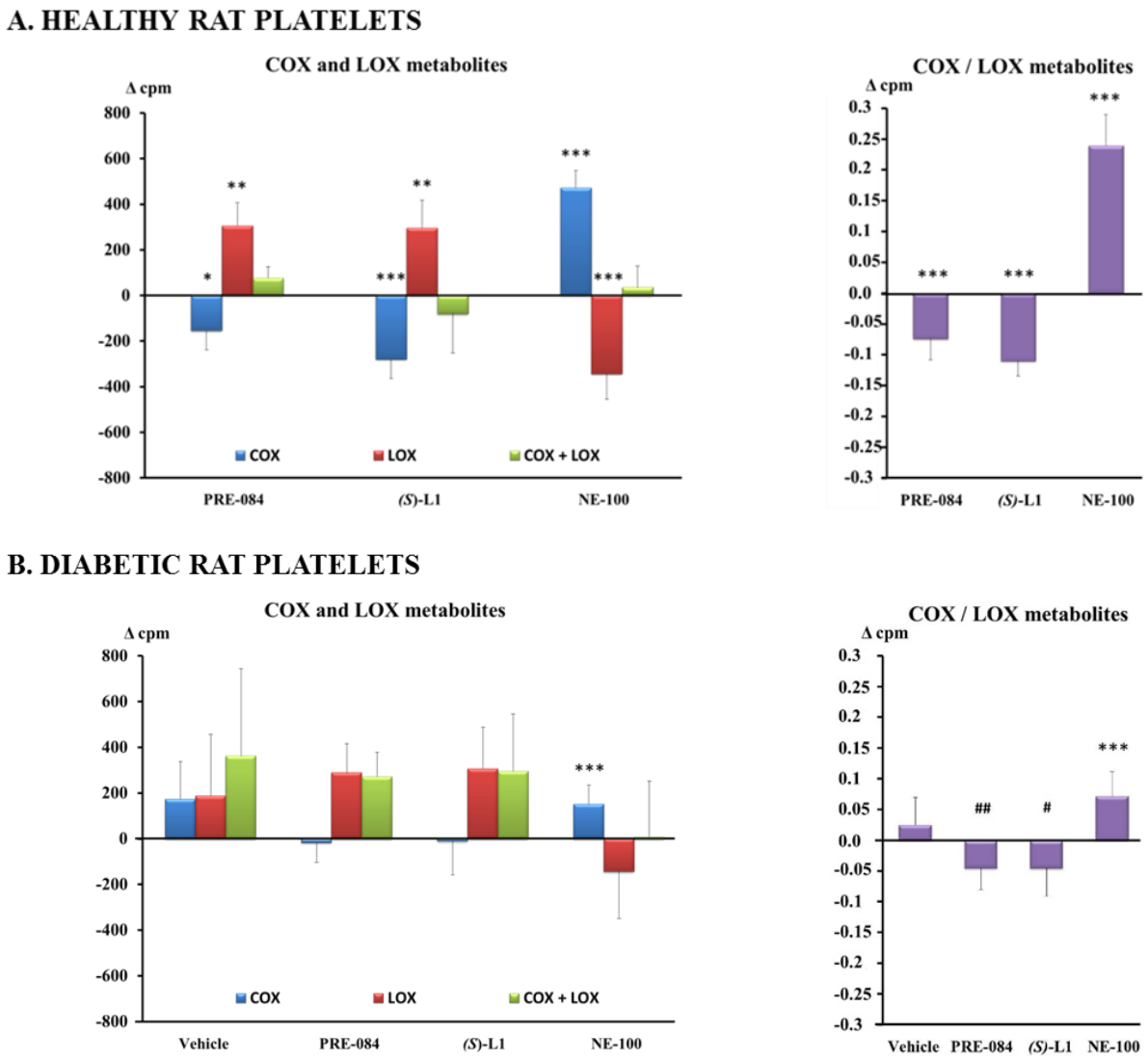

Fig. 10. The *ex vivo* effects of S1R ligands on the radioactive AA metabolism in healthy (A) and diabetic (B) rat platelets

COX, LOX, COX+LOX and COX/LOX levels

(A) ***in the platelets from the healthy*** PRE-084-, *(S)*-L1- or NE-100-treated rats are shown as compared to the vehicle-treated, healthy animals. The zero line in the diagram shows the mean for the isotope activity of the vehicle-treated, healthy rat platelets, while the columns in the figure represent the delta mean ± SD value of the healthy treatment group; n = 9 samples per group; ANOVA, Bonferroni test, $^{*}p < 0.05$, $^{**}p < 0.03$, $^{***}p < 0.01$ compared to the vehicle-treated groups [29].

(B) ***in the platelets from the diabetic*** vehicle-, PRE-084-, *(S)*-L1- or NE-100-treated rats are shown as compared to the vehicle-treated, healthy animals. The zero line in the diagram shows the mean for the isotope activity of the vehicle-treated, healthy rat platelets, while the columns in the figure represent the delta mean ± SD value of the diabetic treatment group; n = 9 samples per group; Welch's ANOVA, Dunnett's T3 test, $^{***}p<0.01$ compared to the vehicle-treated, healthy rats group; $^{\#}p<0.05$, $^{\#\#}p<0.03$ compared to the vehicle-treated, diabetic rat group; cpm: count per minute; COX: total quantity of cyclooxygenase metabolites synthesized from AA in platelets; LOX: total quantity of lipoxygenase metabolites synthesized from AA in platelets [30].

In the healthy rat platelets, the total quantity of vasoconstrictor and platelet aggregator radioactive COX metabolites (CON: sum of $PGF_{2\alpha}$ and TxB_2) was reduced by PRE-084 and *(S)*-L1 but raised by NE-100. The total quantity of vasodilator and anti-aggregator radioactive

COX metabolites (DIL: sum of PGE_2 and PGD_2) was lowered by PRE-084, but it was boosted by NE-100. We can see a significant reduction in the ratio of the CON to DIL metabolites in the *(S)*-L1-treated group (Fig. 11A) [29].

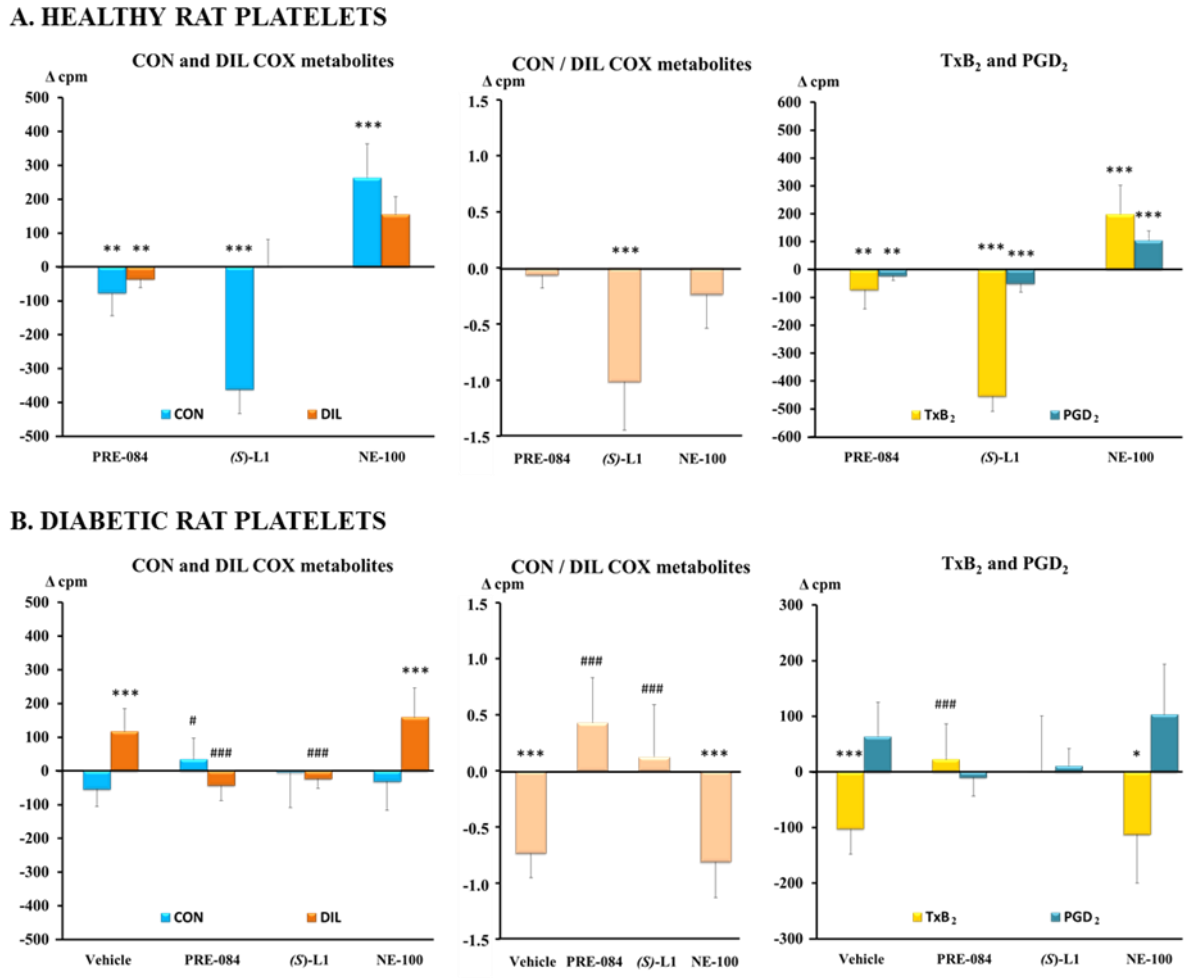

Fig. 11. The *ex vivo* effects of the S1R ligands on the quantity of CON and DIL COX metabolites, the ratio of CON to DIL, the quantity of TxB_2 and PGD_2 of healthy and diabetic rat platelets

CON, DIL, TxB_2 and PGD_2 levels and ration of CON to DIL

(A) ***in the platelets from the healthy*** PRE-084-, *(S)*-L1- or NE-100-treated rats are shown as compared to the vehicle-treated, healthy animals. The zero line in the diagram shows the mean for the isotope activity (or ration) of the vehicle-treated, healthy rat platelets, while the columns in the figure represent the delta mean ± SD value of the healthy treatment group; n = 9 samples per group; ANOVA, Bonferroni test, $^{***}p < 0.01$ compared to the vehicle-treated groups [29].

(B) ***in the platelets from the diabetic*** vehicle-, PRE-084-, *(S)*-L1- or NE-100-treated rats are shown as compared to the vehicle-treated, healthy animals. The zero line in the diagram shows the mean for the isotope activity (or ration) of the vehicle-treated, healthy rat platelets, while the columns in the figure represent the delta mean ± SD value of the diabetic treatment group; n = 9 samples per group; Welch's ANOVA, Dunnett's T3 test, $^{***}p<0.01$ compared to the vehicle-treated, healthy rat group; $^{\#}p<0.05$, $^{\#\#\#}p<0.01$ compared to the vehicle-treated, diabetic rat group; cpm: count per minute; CON: sum of $PGF_{2\alpha}$ and TxB_2; DIL: sum of PGE_2 and PGD_2 [30].

In the healthy platelets, the synthesis of TxB_2 (stable metabolite of TxA_2, the main vasoconstrictor and platelet aggregator product) and the production of PGD_2 (vasodilator and platelet anti-aggregator COX metabolite) were significantly decreased in the PRE-084- and

(S)-L1-treated groups, while they were increased in the NE-100-treated group as compared to the vehicle-treated samples (Fig. 11A) [29].

In the vehicle-treated, *diabetic rat platelets*, the synthesis of CON COX metabolites was not changed significantly, while the quantity of DIL COX products was increased compared to the healthy rat platelets. The quantity of DIL COX metabolites in the diabetic platelets treated with NE-100 was significantly higher than in the healthy platelets from the vehicle-treated rats. The quantity of the CON COX metabolites was raised in the diabetic platelets by the ligand PRE-084 as compared to the vehicle-treated, diabetic platelets. The synthesis of the DIL COX metabolites was reduced not only by PRE-084, but also by *(S)*-L1 compared to the vehicle-treated, diabetic group. In the platelets from the vehicle-treated, diabetic rats, the synthesis of TxB_2 was significantly decreased, while the production of PGD_2, vasodilator and platelet anti-aggregator product was not significantly changed compared to the healthy animals. PRE-084 elevated the synthesis of TxB_2 in diabetic platelets compared to the vehicle-treated, diabetic rat platelets, while NE-100 reduced it compared to the vehicle-treated, healthy rat platelets (Fig. 11B) [30].

Ex vivo analysis of eicosanoid synthesis in platelets by ELISA

We were able to detect both COX-1 and COX-2 enzymes in the platelets of healthy and diabetic rats by ELISA. *In healthy* vehicle-treated *rat platelets*, the concentration of COX-2 was higher than that of COX-1. All of the S1R ligands we tested also increased the levels of COX-1 and COX-2 enzymes in healthy rat platelets. The highest total COX enzyme concentration (COX-1+COX-2) was detected in healthy rat platelets treated with *(S)*-L1 ligand. Which was induced by the greater rise in COX-2 concentration induced by this ligand compared to COX-1. This is supported by the drop in the COX-1/COX-2 ratio and the differential increase in COX-1 and COX-2 concentrations (Fig. 12A) [29].

Constitutive COX-1 concentrations *in diabetic rat platelets* treated with vehicle did not differ significantly from those in healthy platelets treated with vehicle. While the concentration of inducible COX-2 was significantly higher in vehicle-treated diabetic rat platelets, than in vehicle-treated healthy ones. In the platelets of diabetic rats, COX-1 concentrations were increased by PRE- 084 and *(S)*-L1 ligands, whereas COX-2 levels were boosted by all three S1R ligands compared to both vehicle-treated healthy and diabetic rats. The total COX enzyme levels (COX-1+COX-2) *in platelets of diabetic rats* were raised by all three S1R ligands compared to the healthy vehicle-treated group. This was due to a rise in COX-2 levels in the platelets of diabetic animals treated with NE-100 ligand, which was supported by a

drop in the COX-1/COX-2 ratio in NE-100 ligand-treated animals compared to the vehicle-treated healthy and diabetic samples (Fig. 12B) [30].

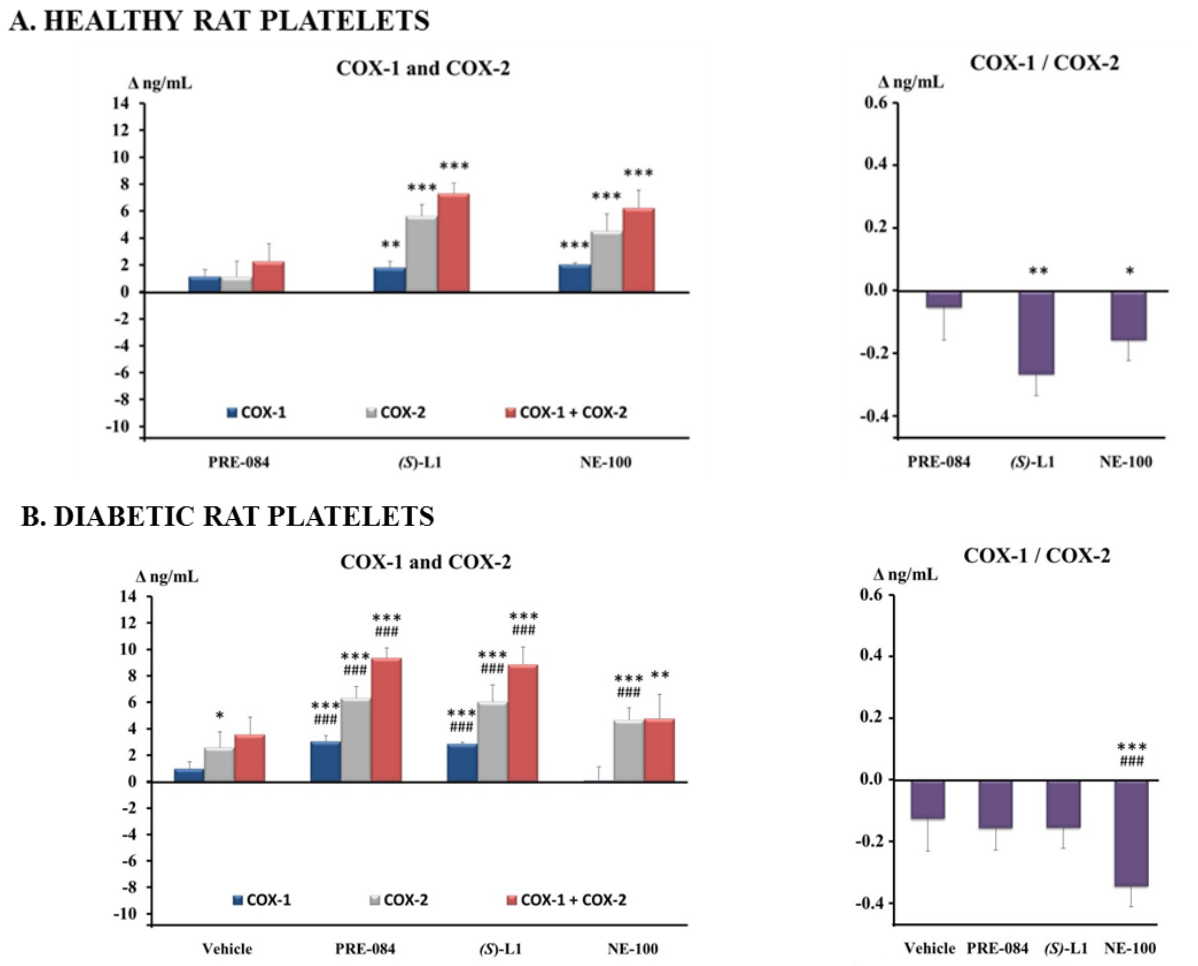

Fig. 12. Effect of S1R ligands on the quantity of COX-1 and COX-2 enzymes in healthy and diabetic rat platelets as determined by ELISA

Concentration of COX-1 and COX-2 enzymes, total quantity of the COX enzymes (COX-1 + COX-2) and COX-1 to COX-2 ratio (COX-1/COX-2)

(A) ***in the platelets from the healthy*** PRE-084-, *(S)*-L1-, or NE-100-treated rats are shown as compared to the vehicle-treated, healthy animals. The zero line in the diagram shows the mean for the concentration or ratio of COX enzymes in the vehicle-treated, healthy rat platelets, while the columns in the figure represent the delta mean ± SD values for the healthy treatment groups; n = 9 samples per group; ANOVA, Bonferroni test, $^{*}p < 0.05$, $^{**}p < 0.03$, $^{***}p < 0.01$ compared to the vehicle-treated groups [29].

(B) ***in the platelets from the diabetic*** vehicle-, PRE-084-, *(S)*-L1-, or NE-100-treated rats are shown as compared to the vehicle-treated, healthy animals. The zero line in the diagram shows the mean for the concentration or ratio of COX enzymes in the vehicle-treated, healthy rat platelets, while the columns in the figure represent the delta mean ± SD values for the diabetic treatment groups; n = 9 samples per group; Welch's ANOVA, Dunnett's T3 test, $^{**}p<0.02$, $^{***}p<0.01$ compared to the vehicle-treated, healthy rat group; $^{\#\#\#}p<0.01$ compared to the vehicle-treated, diabetic rat group; COX-1: Type 1, constitutive cyclooxygenase; COX-2: Type 2, inducible cyclooxygenase [30].

Effects of S1R ligands on S1R and COXs transcripts in healthy and diabetic rat platelets

The mRNA levels of *Sigmar1* were detected in the rat platelet samples using RT-qPCR. The *Sigmar1* mRNA showed a low concentration level *in the healthy rat platelets*. Although the

Ct values were high in most of the cases, we considered them reliable because the RT-qPCR was performed with TaqMan assays. The daily administration of the S1R ligands for one week did not change the level of *Sigmar1* and *Ptgs1* mRNA in the healthy rat platelets (Fig. 13A) [29].

A. HEALTHY RAT PLATELETS

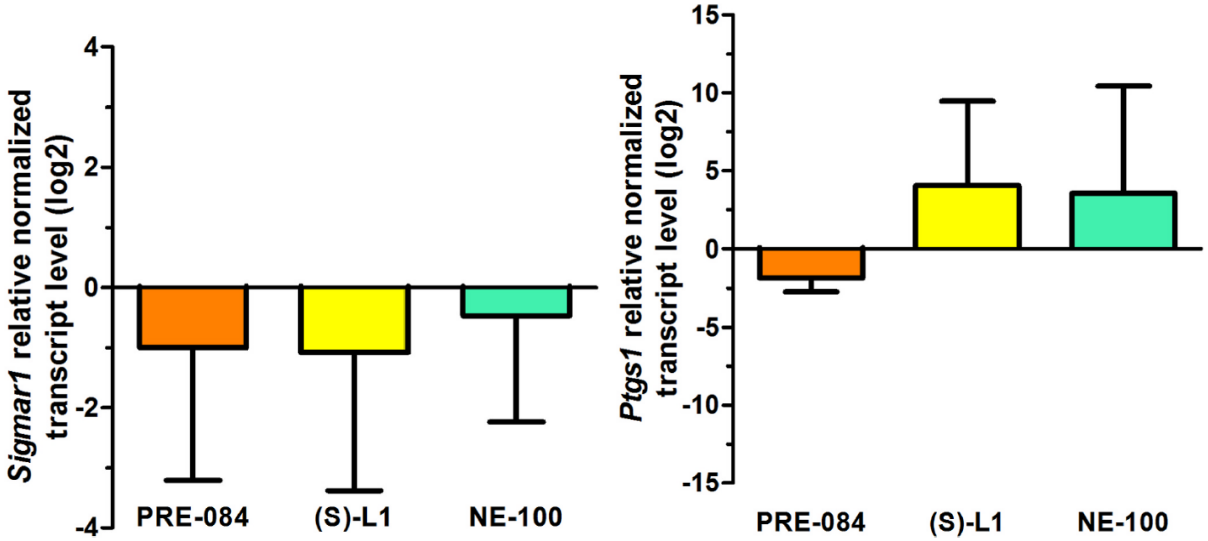

B. DIABETIC RAT PLATELETS

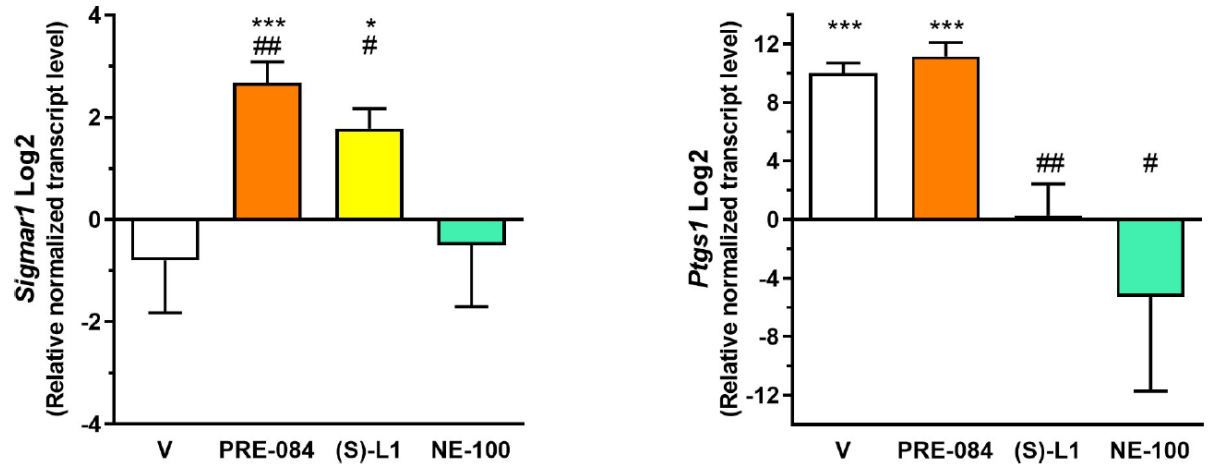

Fig. 13. Effects of S1R ligands on the level of *Sigmar1* and *Ptgs1* transcripts in the healthy and diabetic rat platelets

Relative normalized transcript levels of *Sigmar1 and Ptgs1*

(A) ***in the platelets from the healthy*** PRE-084-, *(S)*-L1-, or NE-100-treated rats are shown as compared to the vehicle-treated, healthy animals. The transcript levels of *Sigmar1* and *Ptgs1* in the rat platelet samples were first normalized to their own endogenous control mRNA levels (*Gapdh*) and then to the similarly normalized mRNA levels in the vehicle-treated animal groups. Fold changes were calculated using the $2^{-\Delta\Delta Ct}$ formula. Mean ± SD, n = 3 samples pooled from nine rats, ANOVA, Dunnett test (Fig. 13A) [29].

(B) ***in the platelets from the diabetic*** vehicle-, PRE-084-, *(S)*-L1-, or NE-100-treated rats are shown as compared to the vehicle-treated, healthy animals. The transcript levels of *Sigmar1* and *Ptgs1* genes in the diabetic rat platelet samples were first normalized to their own endogenous control mRNA levels (*Gapdh*) and then to the similarly normalized mRNA levels in the vehicle-treated, healthy animal group. Fold changes were calculated using the $2^{-\Delta\Delta Ct}$ formula. Mean ± SD, n = 4 representing nine rats per each group, Welch's ANOVA, Dunnett's

T3 test, $^{*}p<0.05$, $^{***}p<0.001$ compared to the vehicle-treated, healthy group; $^{\#}p<0.05$, $^{\#\#}p<0.01$ compared to the vehicle-treated, diabetic group. V: vehicle-treated samples (Fig. 13B) [29,30].

Interestingly, the effect of *(S)*-L1 was different in the case of the *Sigmar1* and *Ptgs1* mRNA levels: an effect similar to the S1R agonist PRE-084 was observed for the *Sigmar1* mRNA level, while a similar effect of the S1R antagonist NE-100 was seen for the *Ptgs1* mRNA concentration in the healthy rat platelets. We measured but did not detect *Ptgs2* mRNA by RT-qPCR in the healthy rat platelet samples using 40 cycles (Fig. 13A) [29].

The mRNA levels of *Sigmar1* were detected ***in diabetic rat platelet*** samples using RT-qPCR. A low concentration level of the *Sigmar1* mRNA was detected in the rat platelets from the vehicle-treated, diabetic animals, similarly to the platelet samples from the healthy rats as published in our previous study [29]. Daily administration of PRE-084 and *(S)*-L1 to diabetic rats for one week elevated *Sigmar1* transcript levels as compared to samples from the vehicle-treated, diabetic or healthy rats [29,30]. The *Sigmar1* mRNA level was lower in the NE-100-treated diabetic group compared to those in the PRE-084 and *(S)*-L1-treated samples but did not differ significantly from the vehicle-treated, diabetic or healthy groups. The level of *Ptgs1* transcript was significantly higher in the platelets of the vehicle-treated, diabetic rats compared to those of the vehicle-treated, healthy animals. In the diabetic rats, PRE-084 treatment did not change *Ptgs1* mRNA levels as compared to samples from the vehicle-treated, diabetic animals. The *Ptgs1* mRNA level was lower in the *(S)*-L1 group than in the vehicle- or PRE-084-treated diabetic rat group but did not differ significantly from the vehicle-treated, healthy group. NE-100 treatment in diabetic rats significantly decreased the platelet *Ptgs1* level as compared to the vehicle-treated, diabetic group. Interestingly, the effect of *(S)*-L1 was different in the case of *Sigmar1* and *Ptgs1* mRNA levels: an effect similar to the S1R agonist PRE-084 was observed for *Sigmar1* mRNA level, while a trend similar to the S1R antagonist NE-100 was seen for the *Ptgs1* mRNA concentration in the rat platelets. *Ptgs2* mRNA was not detected in the platelet samples by RT-qPCR using 40 cycles in the diabetic or healthy rats (Fig. 13B) [29,30].

Ex vivo effects of S1R ligands on healthy and diabetic rat aorta

Analysis of eicosanoid synthesis in abdominal aorta using radioactive AA

Application of the radioactive AA substrate for the study of aortic eicosanoid synthesis. The quantity of radioactive COX metabolites in the rat aorta was significantly reduced by PRE-084, while the quantity of radioactive LOX products was significantly lower in the *(S)*-L1 group, compared to the vehicle-treated group. The quantity of radioactive COX and LOX metabolites in the rat aorta was significantly elevated in the NE-100 group compared to the

vehicle-treated samples. The total quantity of radioactive AA metabolites (COX+LOX) was significantly lower in the PRE-084 and *(S)*-L1 groups but higher in the NE-100 S1R antagonist group compared to the vehicle-treated rat aorta. The COX/LOX ratio of the radioactive AA metabolites in the rat aorta significantly increased in the *(S)*-L1 group compared to the vehicle-treated animals (Fig. 14A) [29].

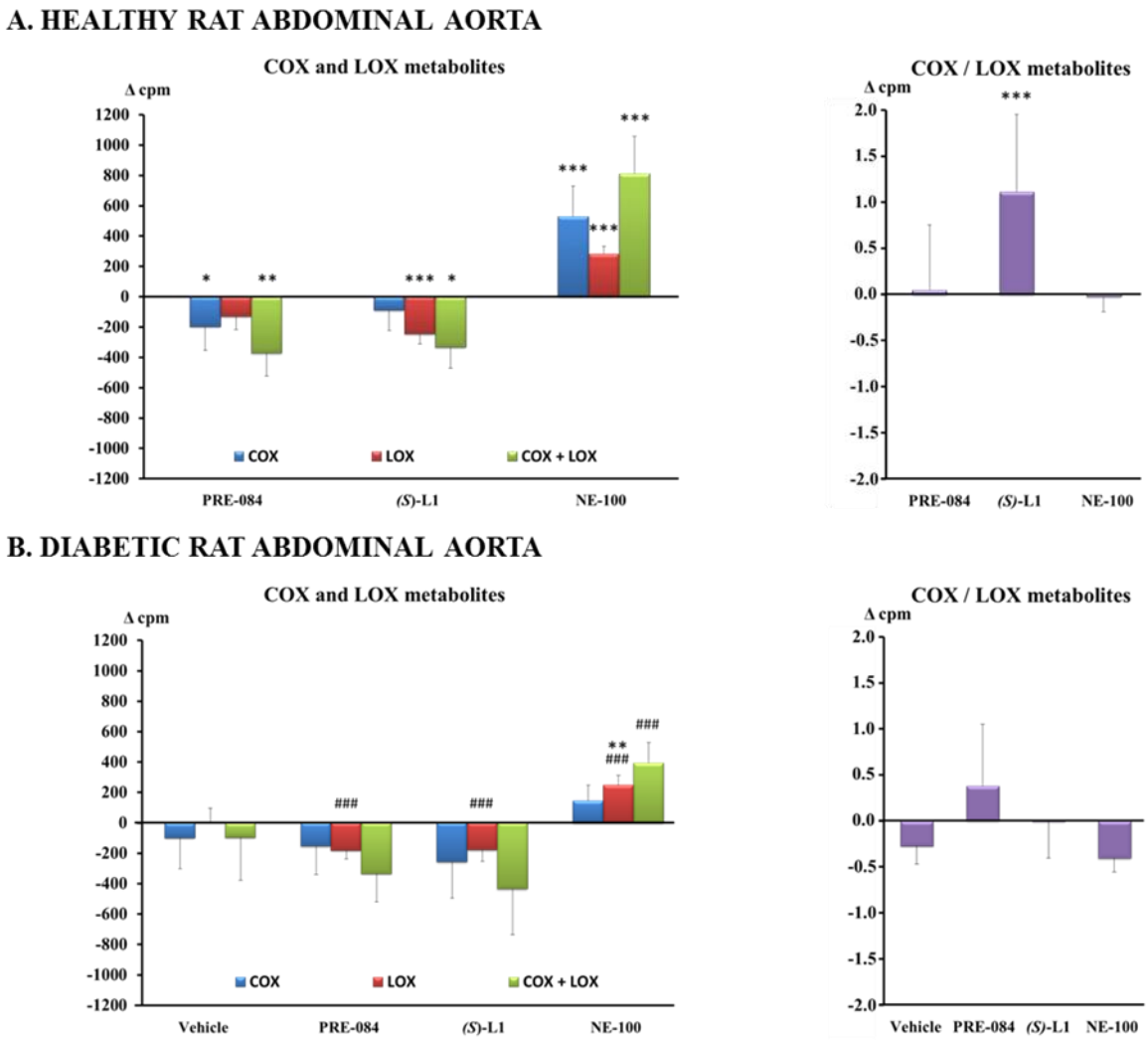

Fig. 14. The *ex vivo* effects of S1R ligands on the radioactive AA metabolism in healthy (A) and diabetic (B) rat abdominal aorta

COX, LOX, COX+LOX and COX/LOX levels

(A) ***in the abdominal aorta from the healthy*** PRE-084-, *(S)*-L1- or NE-100-treated rats are shown as compared to the vehicle-treated, healthy animals. The zero line in the diagram shows the mean for the isotope activity of the vehicle-treated, healthy rat abdominal aorta, while the columns in the figure represent the delta mean ± SD value of the healthy treatment group; n = 9 samples per group; ANOVA, Bonferroni test, $^{*}p < 0.05$, $^{**}p < 0.03$, $^{***}p < 0.01$ compared to the vehicle-treated groups [29].

(B) ***in the abdominal aorta from the diabetic*** vehicle-, PRE-084-, *(S)*-L1- or NE-100-treated rats are shown as compared to the vehicle-treated, healthy animals. The zero line in the diagram shows the mean for the isotope activity of the vehicle-treated, healthy rat aorta, while the columns in the figure represent the delta mean ± SD value of the diabetic treatment group; n = 9 samples per group; Welch's ANOVA, Dunnett's T3 test, $^{**}p<0.03$ compared to the vehicle-treated, healthy rats group; $^{\#\#\#}p<0.01$ compared to the vehicle-treated, diabetic rat

group; cpm: count per minute; COX: total quantity of cyclooxygenase metabolites synthesized from AA in abdominal aorta; LOX: total quantity of lipoxygenase metabolites synthesized from AA in abdominal aorta [30].

The total quantity of metabolites synthesized from AA by COX or LOX enzymes in the aorta samples of the vehicle-treated, diabetic animals did not differ significantly from that of the vehicle-treated, healthy rats. The abdominal aortic AA metabolism (COX+LOX metabolites and COX/LOX product ratio in the vehicle-treated, diabetic rats did not change compared to the vehicle-treated, healthy animals. The synthesis of LOX metabolites was significantly increased in the NE-100-treated, diabetic rat abdominal aorta compared to the vehicle-treated, healthy or diabetic one. PRE-084 and *(S)*-L1 administration reduced the production of LOX metabolites, without modifying the COX pathway in the diabetic aorta compared to the vehicle-treated, diabetic one. The quantity of AA metabolites (COX+LOX) in the diabetic rat abdominal aorta was raised in the NE-100-treated group compared to the vehicle-treated, diabetic animals. The COX/LOX metabolite ratio in the diabetic rat aorta was not modified by any of the S1R ligands compared to the vehicle-treated, healthy or diabetic rats (Fig. 14B) [29,30].

PRE-084 significantly decreased the quantity of DIL radioactive COX metabolites, while NE-100 increased the quantity of both DIL and CON radioactive COX metabolites *in healthy rat aorta* compared to the vehicle-treated group. Overall, NE-100 lowered the CON/DIL ratio of radioactive COX metabolites compared to the vehicle-treated group. In the rat aorta, the synthesis of 6-k-$PGF_{1\alpha}$ (a stable metabolite of prostacyclin and the main vasodilator and platelet anti-aggregator product of the aorta) was significantly increased by *(S)*-L1 and NE-100 and reduced by PRE-084, compared to the vehicle-treated sample. The production of TxB_2 in the healthy rat aorta was significantly lowered by both PRE-084 and *(S)*-L1 but raised by NE-100 (Fig. 15A) [29].

No alterations in CON COX and DIL COX metabolite were detected *in the abdominal aorta of* the vehicle-treated, *diabetic rats* compared to the aorta of the vehicle-treated, healthy animals. The production of CON COX metabolites in the diabetic rat aorta was significantly reduced by *(S)*-L1 compared to the vehicle-treated, healthy and diabetic groups. The synthesis of DIL COX metabolites in the diabetic rat abdominal aorta was stimulated by NE-100 compared to the vehicle-treated, healthy and diabetic samples. Both the *(S)*-L1 and the NE-100 ligands significantly lowered the CON/DIL ratio in the diabetic rat abdominal aorta ring compared to the vehicle-treated, healthy and diabetic samples. The synthesis of the vasoconstrictor TxB_2 was not changed, while the production of 6-k-$PGF_{1\alpha}$ was decreased significantly in the vehicle-treated, diabetic rat aorta compared to the healthy animals. *(S)*-L1

induced the reduction of TxB_2 synthesis in the diabetic aorta compared to the vehicle-treated, healthy and diabetic ones. The NE-100 ligand had opposite effects on these eicosanoids in the diabetic rat abdominal aorta: it reduced the production of TxB_2 compared to the vehicle-treated, healthy rats and increased the synthesis of 6-k-$PGF_{1\alpha}$ compared to the vehicle-treated, healthy and diabetic rats (Fig.15B) [29,30].

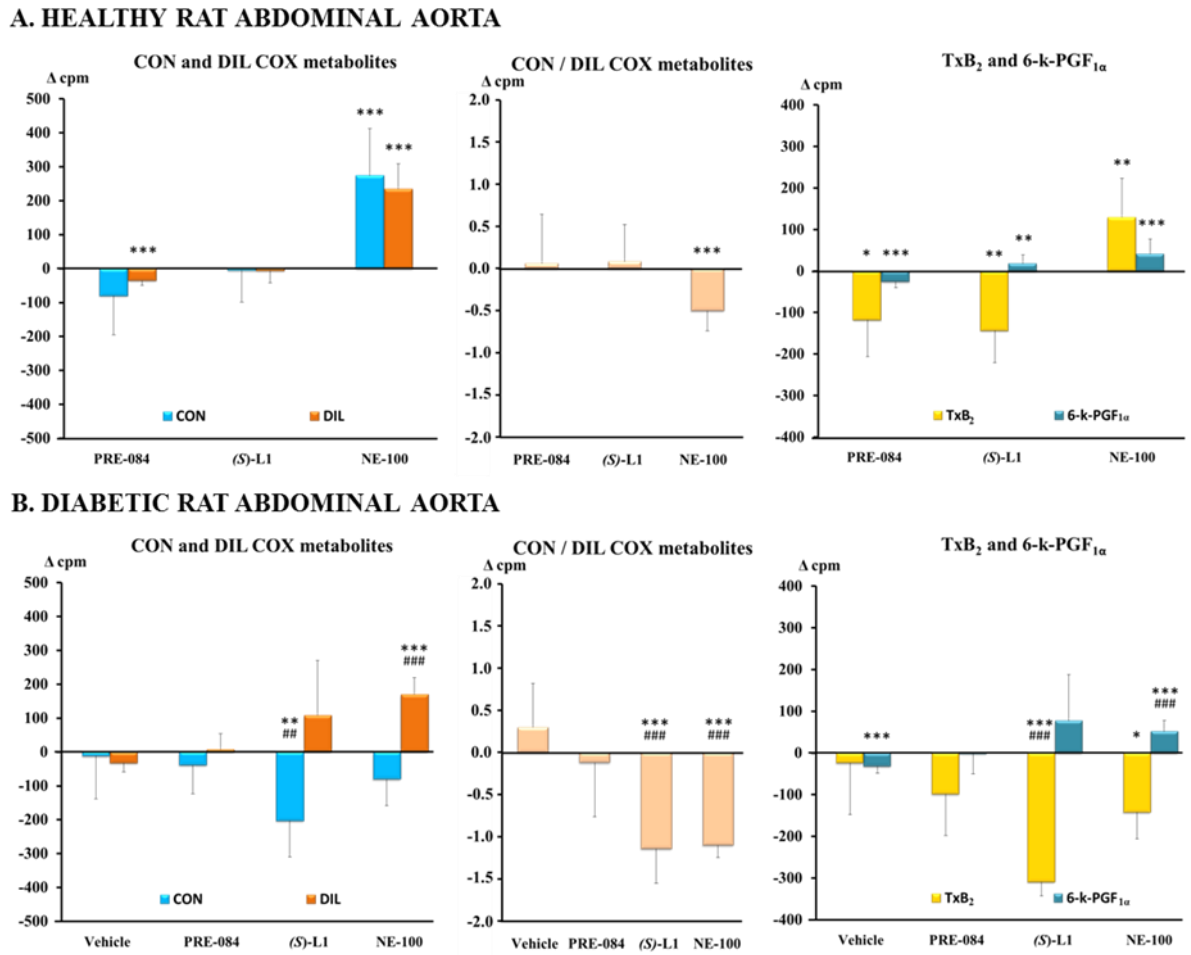

Fig. 15. The *ex vivo* effects of the S1R ligands on the quantity of CON and DIL COX metabolites, the ratio of CON to DIL, the quantity of TxB_2 and 6-k-$PGF_{1\alpha}$ of healthy and diabetic rat abdominal aorta

CON, DIL, TxB_2 and 6-k-$PGF_{1\alpha}$ levels, and ration of CON to DIL

(A) ***in the abdominal aorta from the healthy*** PRE-084-, *(S)*-L1- or NE-100-treated rats are shown as compared to the vehicle-treated, healthy animals. The zero line in the diagram shows the mean for the isotope activity (or ration) of the vehicle-treated, healthy rat aorta, while the columns in the figure represent the delta mean ± SD value of the healthy treatment group; n = 9 samples per group; ANOVA, Bonferroni test, $^{*}p<0.05$, $^{**}p<0.03$, $^{***}p<0.01$ compared to the vehicle-treated groups [29].

(B) ***in the abdominal aorta from the diabetic*** vehicle-, PRE-084-, *(S)*-L1- or NE-100-treated rats are shown as compared to the vehicle-treated, healthy animals. The zero line in the diagram shows the mean for the isotope activity (or ration) of the vehicle-treated, healthy rat aorta, while the columns in the figure represent the delta mean ± SD value of the diabetic treatment group; n = 9 samples per group; Welch's ANOVA, Dunnett's T3 test, $^{*}p<0.05$, $^{**}p<0.03$, $^{***}p<0.01$ compared to the vehicle-treated, healthy rat group; $^{\#\#}p<0.03$, $^{\#\#\#}p<0.01$ compared to the vehicle-treated, diabetic rat group; cpm: count per minute; CON: sum of $PGF_{2\alpha}$ and TxB_2; DIL: sum of 6-k-$PGF_{1\alpha}$ (which is a stable metabolite of prostacyclin), PGE_2 and PGD_2 [[30].

Analysis of eicosanoid synthesis in healthy and diabetic rat aorta by ELISA

We detected a higher concentration of COX-2 than COX-1 in *the healthy rat abdominal aorta*. PRE-084 and *(S)*-L1 increased the aortic COX-1 and COX-2 concentrations, with a higher elevation observed for COX-1. NE-100 reduced the COX-2 level and therefore the balance between the enzymes shifted to COX-1. The most effective S1R ligand was *(S)*-L1, which increased the level of COX-1 and COX-2 (Fig. 16A) [29].

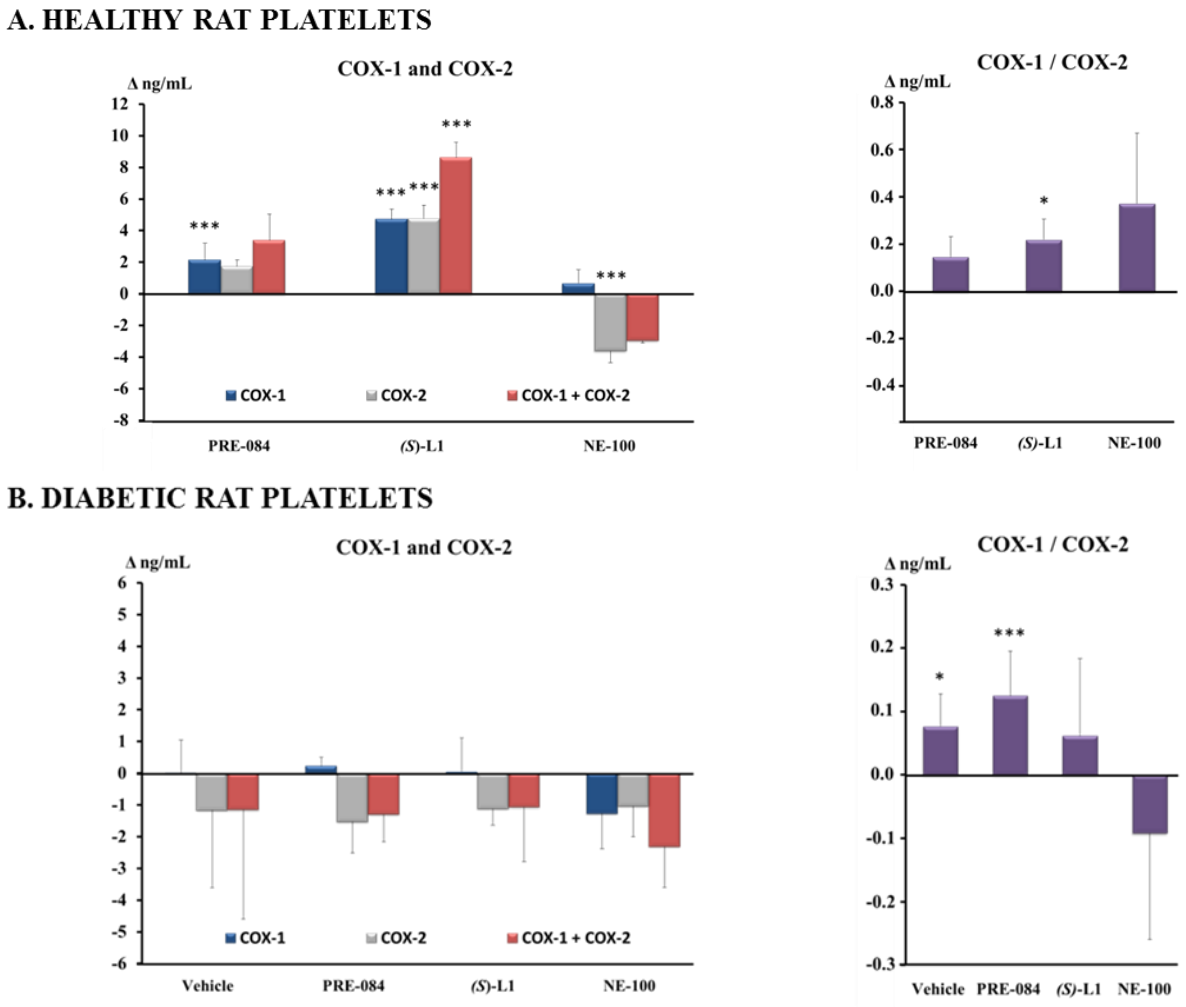

Fig. 16. Effect of S1R ligands on the quantity of COX-1 and COX-2 enzymes in healthy and diabetic rat abdominal aorta as determined by ELISA

Concentration of COX-1 and COX-2 enzymes, total quantity of COX enzymes (COX-1 + COX-2) and the COX-1 to COX-2 ratio (COX-1/COX-2)

(A) ***in the abdominal aorta from the healthy*** PRE-084-, *(S)*-L1-, or NE-100-treated rats are shown as compared to the vehicle-treated, healthy animals. The zero line in the diagram shows the mean for the concentration or ratio of COX enzymes in the vehicle-treated, healthy rat aorta, while the columns in the figure represent the delta mean ± SD values for the healthy treatment groups; n = 9 samples per group; ANOVA, Bonferroni test, $^{*}p < 0.05$, $^{***}p < 0.01$ compared to the vehicle-treated groups [29].

(B) ***in the abdominal aorta from the diabetic*** vehicle, PRE-084-, *(S)*-L1-, or NE-100-treated rats are shown as compared to the vehicle-treated, healthy animals. The zero line in the diagram shows the mean for the concentration or ratio of COX enzymes in the vehicle-treated, healthy rat aorta, while the columns in the figure represent the delta mean ± SD values for the diabetic treatment groups; n = 9 samples per group; Welch's ANOVA, Dunnett's T3 test, $^{*}p<0.05$, $^{***}p<0.01$ compared to the vehicle-treated, healthy rat group; $^{\#}p<0.05$

compared to the vehicle-treated, diabetic rat group; COX-1: Type 1, constitutive cyclooxygenase; COX-2: Type 2, inducible cyclooxygenase [30].

The concentration of COX-2 in the aorta of *diabetic* vehicle-treated rats was also higher than that of COX-1, similar to that of healthy abdominal aorta. Neither the concentration of COX-1 or COX-2 nor their sum (COX-1 + COX-2) in the aorta of the vehicle-treated, diabetic rats showed significant differences compared to vehicle-treated, healthy animals. In the aorta of diabetic rats, the concentrations of these parameters were not altered by any of the S1R ligands we tested. However, the COX-1/COX-2 ratio in the aorta of diabetic rats treated with vehicle or PRE-084 was significantly higher than in healthy rats treated with vehicle (Fig.16B) [29,30].

DISCUSSION

The presence of S1R and its role in physiological and pathological processes have been shown in several cell types (parenchymal cells, microglial cells, macrophages, lymphocytes and endothelial cells) [5,6,15,50], but its presence and role in platelets have not yet been studied. Intracellularly, S1R is mainly found in the MAM of the ER, but is able to migrate from the ER to the plasma membrane [2,6]. Platelets are anuclear cells, but they also have many other intracellular cellular components, such as dense granules, α-granules, lysosomes, dense tubular systems, Golgi apparatus, ER and mitochondria [51]. All these structural features provide a possibility for the presence of S1R in platelets. Although platelets do not have a nucleus, they are capable of protein biosynthesis using megakaryocyte-derived cytoplasmic mRNA [52]. Based on these data, we were able to confirm our hypothesis that non-activated rat platelets are also capable of S1R expression at the mRNA and protein levels using RT-PCR, qPCR and immunocytochemistry (Fig. 3 and 4) [31]. Platelets are involved not only in haemostasis, but also, together with white blood cells (macrophages, lymphocytes and granulocytes), in the body's defence responses, such as inflammation, and in innate and acquired immunity [19,53,54]. Agonists of platelet receptors induce platelet activation, i.e., deformation, adhesion, degranulation, aggregation, receptor expression and AA metabolism, through various intracellular signalling pathways [9,55–57]. ADP released from the platelet granule itself also contributes to AA-induced platelet activation [58].

Through the intracellular membrane-bound localization of S1R, it regulates several intracellular processes (such as ROS reduction, elimination of pathogenic proteins, ATP production, modulation of ion channels, intracellular lipid transport and enzyme activation) [15,59–64].

Since the role of S1R in modifying membrane structure and function has been studied extensively [59] and we detected S1R in platelets in the present experiment, we hypothesized that the S1R agonist PRE-084 may affect the metabolism of membrane PLs to AA and eicosanoids in non-activated rat platelets *in vitro*.

In order to prevent spontaneous platelet activation and to correctly interpret the effect of S1R ligands, we had to observe several experimental conditions during our experiments. Age dependence of platelet structure and function [65] and hormone dependence of AA metabolism [66,67] are already known, so we investigated platelet function in sex- and age-matched male rats. Following literature recommendations, functional platelet analysis was performed within one hour of sample collection, both when using whole blood [45,68] and when using separated platelets [69]. The choice of anticoagulant for whole blood aggregometry (MEA) was based on the recommendation of the device manufacturer (Roche Ltd., Budapest, Hungary) and the need to prevent a decrease in physiological Ca^{2+} concentration, which is essential for platelet aggregation [55–57]. In addition, the use of a calcium chelating anticoagulant could interfere with the study of the effects of S1R ligands that can influence intracellular calcium ion homeostasis [2,5,6,59,70]. Based on these criteria, we chose hirudin, which does not form calcium chelate [68,71]. To study the effect of S1R ligands on platelet AA metabolism *in vitro* and *ex vivo*, we had to prevent spontaneous platelet activation. In order to prevent platelet activation during platelet separation, we used plastic devices, a thick needle to drain blood, and EDTA, a calcium chelating anticoagulant that inhibits platelet aggregation. To investigate platelet eicosanoid synthesis, we used EDTA- and plasma protein-free tissue culture medium (Medium 199), which provided the Ca^{2+} concentration required for physiological platelet function. In order to exclude platelet activation, the concentration of the radioactive substrate used as a marker (0.172 nM 1-^{14}C-AA) was significantly lower than the quantity of the aggregation inducer AA (0.5 mM) [29–31].

In vitro pre-treatment with the S1R agonist PRE-084 enhanced AA metabolism of non-activated platelets from healthy 12-week-old male rats, which was detected semi-quantitatively using a radioactive substrate (Fig. 5) and quantitatively by ELISA (Fig. 6) [31]. This effect may be explained by the fact that PRE-084 increased the PL content of the cell membrane through its intracellular lipid transport effect, while its phospholipase-activating ability elevated the quantity of free AA, the substrate of eicosanoids, by inducing PL deacylation [9,59,60]. Although both the total quantity of AA metabolites formed via the COX pathway (Fig. 5A) and the total quantity of AA metabolites formed via the LOX

pathway (Fig. 5B) rose *in vitro* upon PRE-084 treatment, the rate of increase and the dose-dependence of the increase were not identical [31]. These results suggest the possibility that this S1R ligand may stimulate the expression and/or activity of COX and LOX directly, in addition to raising the level of free AA. The differential effects of PRE-084 ligand on COX and LOX expression and/or activity can be explained by the different exposure times and the different sensitivity of the enzymes [72]. Several isoforms of the cyclooxygenase enzyme are known, one of which is the constitutively expressed COX-1, while the other is the inducible COX-2 isoenzyme. Although platelets are anuclear cells, they are able to synthesize COX-1 *de novo* from cytoplasmic mRNA originating from megakaryocytes [73]. Hu and colleagues have also detected COX-2 mRNA and protein in human platelets, but at significantly lower levels than COX-1 enzyme mRNA and protein [74]. In our preliminary experiments, growth in COX-1 concentration was detected by ELISA in non-activated rat platelets after *in vitro* PRE-084 treatment (Fig. 6), which is consistent with the increase in the total quantity of COX metabolites obtained using the radioactive substrate. Under our present experimental conditions, the synthesis of individual COX products (TxB_2, Fig. 5C; PGD_2, Fig. 5D; PGE_2, Fig. 5E) was increased, but to different degrees [31]. These results suggest that, in non-activated platelets, *in vitro* pre-treatment with PRE-084 can probably enhance not only the expression and/or activation of PLA_2, COX and LOX enzymes, but also specific enzymes involved in the formation of eicosanoids synthesized by the COX pathway. At present, the exact mechanism of these effects is not yet known, although several studies have reported that S1R is able to modulate the function of a number of ion channels and enzymes [2,5,6,16,70]. In the presence of PRE-084, non-activated rat platelets synthesized more aggregating and vasoconstrictor TxA_2 stable metabolites, i.e., TxB_2 (Fig. 5C, 6), anti-aggregator and vasodilator PGD_2 (Fig. 5D), and significantly higher quantities of PGE_2 (Fig. 5E) [31], whose effects on platelets are concentration-dependent [9]. In addition to these experimental results, in order to clarify the effect of PRE-084 on platelet aggregation, we investigated the direct effect of this S1R ligand on ADP- and AA-induced platelet aggregation. Concentrations of PRE-084 (Fig. 5), which enhance eicosanoid synthesis in non-activated platelets, boosted both ADP- and AA-induced platelet aggregation (Table 1) using whole blood aggregometry [31]. In this procedure, fibrinogen, calcium ion and other circulating blood elements that promote platelet aggregation are also present. The effect of S1R agonist on the speed of AA-induced aggregation was most pronounced (Table 1) compared to the control group [31]. This may be explained by the fact that AA-synthesized thromboxane, when bound to its own receptors, induces autocrine and paracrine platelet activation, and AA-induced platelet activation

induces endogenous (granule-derived) ADP inducer release [58]. The dose-response curve of PRE-084 on platelet aggregation induced by ADP or AA did not differ significantly (Table 1) [31], despite the fact that the primary effect of ADP on platelets is receptor-mediated, whereas the primary effect of AA is not. However, their secondary intracellular signalling pathways are similar, as both are able to induce a rise in $[Ca^{2+}]_i$ and the secretion of endogenous inducers, such as thromboxane, serotonin and ADP [19,23,75]. It was hypothesized that PRE-084 might modulate this common intracellular signalling pathway of ADP and AA. However, the magnitude of the increase in platelet aggregation induced by PRE-084 (Table 1) was smaller than that of thromboxane production (Fig. 5C and 6). This difference can be explained by the greater formation of anti-aggregator eicosanoids (PGD_2, Fig. 5D and PGE_2, Fig. 5E) [31] and the simultaneous presence of PRE-084-binding cells and plasma proteins. However, the mechanism of these latter processes and their presence in platelets is not yet clearly understood.

Following the demonstration of *in vitro* rat platelet AA metabolism (Fig. 5 and 6) and the aggregation (Table 1) enhancing effects of the S1R agonist PRE-084 [31], we extended our studies to other S1R ligands, such as NE-100, known as an S1R antagonist, and a novel ligand, *(S)*-L1. The platelets and the endothelial cell layer lining the inner surface of blood vessels form a functional unit [76–78]. Under physiological conditions, the AA metabolism of platelets and endothelial cells is known to differ significantly. Platelets primarily produce the vasoconstrictor thromboxane, which induces platelet aggregation, and the endothelium primarily produces the inhibitory vasodilator prostacyclin; however, under physiological conditions, these products are in equilibrium and thus ensure physiological microcirculation [47,76,77,79,80].

Based on this knowledge, we investigated the *in vivo/ex vivo* effects of the S1R ligands noted above on platelet and aortic eicosanoid synthesis following sub-chronic i.p. treatment in both healthy and STZ-induced diabetic 16-week-old male rats.

The S1R ligands to be applied were selected based on their binding strength to the receptor and the binding site in the S1R binding pocket (Fig. 7). The main difference between S1R agonist and antagonist binding is whether the ligand can interact with the C-terminal helix of S1R. The cyclohexane ring of PRE-084 is the only moiety that can interact with this helix [49]. *(S)*-L1, has a very similar binding position to the S1R antagonist NE-100 [29,30,39]. The duration of treatment was determined by the platelet lifetime (one week) [81,82]. We confirmed that all S1R ligands administered i.p. were taken up into the circulation, but their 30 min serum levels showed a large variance, which may indicate a difference in their

absorption rate. The difference observed in the time-dependent analysis of the serum levels of the ligands (Fig. 8) [29] could be explained by the different metabolism and excretion of the ligands, the mechanism of which is not yet fully understood. To exclude the direct effect of S1R ligands, our *ex vivo* studies were started 20 h after the last ligand treatment, when the serum levels of the ligands were already below the limit of detection or quantification (Table 2) [29]. Thus, the changes in platelet and aortic AA metabolism induced by S1R ligands and detected *ex vivo* may be due to ligand-induced effects on platelet and aortic function *in vivo*.

In vivo, none of the S1R ligands we tested resulted in changes in the total quantity of radioactive AA metabolites in healthy rat platelets *ex vivo*. Nevertheless, a decrease in the COX/LOX ratio was detected in platelets in response to PRE-084 and *(S)*-L1, whereas a rise in this ratio was detected in response to NE-100 (Fig. 10A). In healthy rat aorta, however, the total quantity of AA metabolites was lowered by PRE-084 and *(S)*-L1, whereas NE-100 raised it. In addition, a product shift towards the COX pathway within the AA cascade was observed upon *(S)*-L1 treatment (Fig. 14A). In healthy rat platelets, none of the ligands induced changes in either S1R or COX mRNA levels; that is the difference in AA metabolism cannot be explained by the effect of the ligands on S1R or COX enzyme transcription (Fig. 13A) [29]. Although platelets are non-nucleated cells, they are nevertheless able to synthesize constitutive COX-1 *de novo* from cytoplasmic mRNA from megakaryocytes [73]. Hu et al. (2017) have also detected COX-2 mRNA and protein in human platelets, though in smaller quantities [74]. However, under our current experimental conditions, we were unable to detect COX-2 (*Ptgs2*) mRNA in rat platelets by 40-cycle RT-qPCR. This may be explained by the fact that a limited pool of mRNA transcripts from megakaryocytes can be used for protein (e.g. COX-2) synthesis, and thus increased AA metabolism may lead to depletion of intracellular reserves (mRNA, enzyme pool and $[Ca^{2+}]_i$). Although *in vivo* treatment with PRE-084 and *(S)*-L1 decreased the total quantity of radioactive COX metabolites in platelets of healthy rats and NE-100 increased it (Fig. 10A). We did not detect any change in COX enzyme (COX-1+COX-2) concentrations by ELISA, after treatment with PRE-084, whereas an increase was observed with *(S)*-L1 and NE-100 treatment. Both *(S)*-L1 and NE-100 raised the concentration of platelet COX-1 and COX-2 enzymes, but the drop in the COX-1/COX-2 ratio for both ligands suggests that their effect on COX-2 was greater than that of COX-1 (Fig. 12A) [29]. Therefore, the fall in the total quantity of radioactive AA metabolites formed by the COX pathway (Fig. 10) in healthy rat platelets following *in vivo* treatment with PRE-084 and *(S)*-L1 [29] can be explained by inhibition of the COX enzyme or by a drop in the absolute or relative quantity of free AA substrate. The formation of AA metabolites depends

on the presence of sufficient quantities of free AA, which may be influenced by the PL composition of the membrane, phospholipase activity and $[Ca^{2+}]_i$ levels. S1R is known to be able to modulate all these factors [6,9,60,83]. Since the total quantity of AA metabolites (COX+LOX) in healthy rat platelets was not reduced by either PRE-084 or *(S)*-L1 treatment *in vivo* (Fig. 10A) [29], an absolute reduction in free AA can be excluded. Therefore, in this case, the drop in the total quantity of COX metabolites could be caused by a direct inhibition of COX and/or a rise in LOX activity, i.e., a relative fall in the AA substrate, as supported by the reduction in the COX/LOX ratio (Fig. 10A) [29]. Although no data are available on the direct effects of S1R ligands on COX activity, a recent lipidomic study found downregulation of the COX pathway by bufotenin, an S1R ligand [16]. In contrast to the PRE-084 ligand, both *(S)*-L1- and NE-100-treatment showed a rise in COX enzyme concentration in platelets from healthy rats by ELISA (Fig. 12A). However, *(S)*-L1 decreased the formation of radioactive COX metabolites, whereas NE-100 enhanced it (Fig. 10A) [29]. This could be explained by the difference in the effect of each ligand on the translation, synthesis and/or activation of COX and specific enzymes involved in the synthesis of eicosanoids. *In vivo* treatment with each S1R ligand induced different degrees and/or directions of changes in COX-mediated metabolites in healthy rat platelets, suggesting that ligands act not only through the PL, COX and LOX, but also through the influence of specific enzymes. For example, *(S)*-L1 treatment led to a decrease in CON/DIL ratio by reducing the synthesis of CON products. The synthesis of the major COX metabolite in platelets, the vasoconstrictor and platelet aggregator thromboxane, was reduced much more by our new ligand *(S)*-L1 than by PRE-084 (Fig. 11A) [29].

The effects of our S1R ligands on AA metabolism in healthy rat aorta were significantly different compared to their effects on platelets. S1R ligands resulted in a similar direction but smaller changes in the total quantity of COX metabolites in healthy rat aorta (Fig. 14A) compared to platelets (Fig. 10A) [29]. In contrast to platelets (Fig. 10A), the total quantity of eicosanoids formed by the aorta via the LOX pathway was lowered by *(S)*-L1, whereas NE-100 raised it (Fig. 14A) [29]. These changes can be explained by changes in both the absolute and relative quantities of AA substrate. In the aorta, the decrease in the total quantity of AA metabolites (COX+LOX) due to *(S)*-L1 and PRE-084 and the increase of it due to NE-100 suggest that S1R ligands may have affected the release of AA from PLs, i.e., the absolute quantity of substrate. On the other hand, growth in the ratio of COX to LOX metabolites (COX/LOX) in the aorta in response to *(S)*-L1 points to a dominance of the COX pathway, resulting in a relative substrate depletion for LOX enzymes (Fig. 14A). Although the effects

of ligands on the total quantity of platelet (Fig. 10A) and aortic COX metabolites were similar (Fig. 14A), their effects on the ratio of vasoconstrictor to platelet aggregator (CON) and vasodilator to platelet anti-aggregator COX metabolites (DIL) (CON/DIL) formed by the COX pathway differed significantly. *(S)*-L1 produced a drop in CON/DIL in platelets (Fig. 11A), whereas NE-100 led to a flow in CON/DIL in aorta (Fig. 15A). In aorta, NE-100 lowered the CON/DIL ratio despite increasing the synthesis of both CON and DIL metabolites. The synthesis of the major COX metabolite in the aorta, the vasodilator and anti-aggregator prostacyclin was increased by the novel ligand we tested, *(S)*-L1, which was inhibited by PRE-084 (Fig. 15A) [29].

The neuro- [6] and cardio-protective [84] effects of S1R have already been demonstrated. However, only a fraction of cardiovascular diseases is of cardiac origin, and macro- and microvascular dysfunction and/or platelet activation are responsible for the development and exacerbation of many diseases. Eicosanoids are *de novo*, locally formed [73], short half-life [9,85], autocrine, paracrine and endocrine [9] AA metabolites. Under physiological conditions, the balance of vasoactive and platelet-activating COX products synthesized by platelets and vascular endothelium ensures proper microcirculation and tissue perfusion [22,80]. Sub-chronic *in vivo* administration of the ligands PRE-084, *(S)*-L1 and NE-100 S1R in healthy rats modulated both rat platelet and aortic eicosanoid synthesis; however, these effects were cell/tissue-specific. The S1R ligands we tested resulted in a predominance of vasodilator and platelet aggregation inhibitory COX eicosanoids in healthy rat platelets and aorta. Under our present study conditions, *(S)*-L1 was found to be the most potent of the S1R ligands we tested in maintaining the balance of platelet and vascular eicosanoid synthesis, i.e., tissue perfusion and microcirculation.

Diabetes is a chronic, progressive inflammatory disease characterized by abnormal carbohydrate, lipid and protein metabolism. These abnormalities lead to the formation of AGE, accumulation of ROS, endothelial dysfunction and platelet activation [17,18]. Cytokines and eicosanoids synthesized by impaired endothelium and activated platelets play a role in both the development and progression of atherosclerosis. S1R, which modulates cell function [1,15,16], is expressed on both endothelial cells [50] and platelets [31].

It is well established in the literature that S1R gene expression reduces the production of inflammatory cytokines [10], reactive oxygen species and advanced glycation end products [18,27,86], as well as abnormal protein accumulation in diabetes, and protects against the development of diabetic complications [14].

Based on all this knowledge, we considered it important to investigate the effects of sub-chronic *in vivo* S1R ligand treatment on *ex vivo* eicosanoid synthesis in platelets and abdominal aorta of STZ-induced diabetic rats. We chose STZ-induced diabetes mellitus as a reliable, reproducible model of chronic inflammation and oxidative stress in which the development and time course of complications can be easily monitored [79]. STZ contains glucose and N-methyl-N-nitrosourea groups [87]. The binding of its glucose component to glucose transporter-2 (GLUT-2) promotes the entry of STZ into pancreatic, liver and renal tubule epithelial cells with GLUT-2 [88,89]. STZ as a constituent of N-methyl-N-nitrosourea delivered to cells in this way induces DNA methylation [90], alkylation [91] and oxidation [92]. These processes induce cell apoptosis, leading to the development of diabetes mellitus and liver and kidney damage. Ha et al. (2012) reported a protective role of S1R against pathological changes in STZ-induced diabetes mellitus [14]. Since both platelets and endothelial cells are involved in the development of diabetic complications [86,93], we hypothesized that S1R ligands may modulate the function of both cell types. Sub-chronic, *in vivo* treatment with S1R ligands was also able to alter platelet and aortic AA metabolism in STZ-induced diabetic rats despite the absence of ligands in the blood at the time of *ex vivo* study (Fig. 10B and 14B). However, under our current experimental conditions, we did not detect *Ptgs2* mRNA by RT-qPCR either in the platelets of the healthy controls [Fig. 13A] or in the diabetic rats [Fig. 13B]. We detected unchanged *Sigmar1* and increased *Ptgs1* transcript levels in the platelets of the diabetic rats treated with vehicle compared to the healthy rats (Fig. 13B) [29]. These results do not support our hypothesis that *Sigmar1* transcript expression is increased in platelets from vehicle-treated diabetic rats. However, under pathological conditions, the S1R agonist PRE-084 [94] with antioxidant capabilities and the novel SR-1 ligand *(S)*-L1 were able to increase S1R transcript levels (Fig. 13B), which may play a protective role against oxidative stress in diabetes. NE-100 decreased *Ptgs1* compared to the vehicle-treated diabetic group (Fig. 13B). These results support our hypothesis that PRE-084 S1R agonist and NE-100 antagonist have opposite effects on platelet *Sigmar1* and *Ptgs1* transcript levels. The structural similarity between *(S)*-L1 and NE-100 is only reflected in a similar effect on platelet *Ptgs1* levels (Fig. 13B), suggesting that the modulatory effect of S1R ligands is enzyme-, cell- and tissue-specific [30]. In the platelets of diabetic rats, we observed an increase in DIL COX products and a decrease in the CON/DIL ratio (Fig. 11B) compared to healthy animals, while in the aorta we observed a decrease in 6-k-$PGF_{1\alpha}$ synthesis (Fig. 15B) [30]. These results support our hypothesis that platelet and endothelial cell activation *in vivo* can be detected *ex vivo*. In platelets, we observed a change that was the

opposite of what was expected, which could be the result of a smaller platelet storage pool (e.g. i.c. Ca^{2+}) due to *in vivo* platelet activation or a compensatory mechanism during the early stages of diabetes. In previous *ex vivo* studies of platelet aggregation in STZ-induced diabetic rats, we did not detect an enhanced platelet aggregation readiness either [47]. Scridon et al. (2019) reported high intrinsic platelet activity and low *in vitro* ADP- and AA-induced platelet aggregation in STZ-induced diabetic animals compared to a non-diabetic control group. These paradoxical results suggest that an inhibitory factor is present in the plasma of diabetic rats to counteract (or even exceed) the increased intrinsic platelet activity, the quantity and extent of which may vary with disease progression [95]. These data support our results.

Treatment with PRE-084 and *(S)*-L1 ligands did not affect the total quantity of radioactive eicosanoids (COX+LOX) synthesized by platelets from diabetic rats, but reduced the COX/LOX ratio. These results suggest that PRE-084 and *(S)*-L1 induce a shift in platelet AA metabolism towards the LOX pathway without altering the quantity of AA substrate released from PLs (Fig. 10B). Although PRE-084 and *(S)*-L1 did not elevate COX-1 mRNA (Fig. 13B) in diabetic platelets compared to vehicle-treated diabetic platelets, they did increase COX enzyme concentrations as determined by ELISA (Fig. 12B). This did not, however, result in a rise in the total quantity of COX pathway products (Fig. 10B), i.e., an increase in COX enzyme activity. However, it did modulate the function of enzymes involved in the synthesis of individual COX products, such that their function resulted in a normalization of the changes measured in diabetic platelets (Fig. 11B). For example, in diabetic rats, higher CON/DIL ratios were observed in the platelets of PRE-084- and *(S)*-L1-treated animals, indicating a predominance of CON COX metabolites (Fig. 11B) compared to the platelets of vehicle-treated diabetic rats, which in turn showed a reduced CON/DIL ratio compared to the vehicle-treated healthy group [30].

Although a number of safety procedures were used to prevent spontaneous platelet aggregation during platelet isolation and *in vitro* studies and no direct platelet aggregation was induced in *ex vivo* studies, activation of platelet intracellular signalling pathways cannot be completely excluded. The EDTA used in platelet isolation reduced the e.c. available to platelets. Ca^{2+} available to platelets, which was normalized by the tissue culture medium used in the *ex vivo* study (Medium 199). In our *ex vivo* study, since the tissue culture medium did not contain fibrinogen, platelet aggregation could not occur. One limitation of our study is that we did not examine a platelet population at resting state, but one adapted to changes in the medium environment with physiological parameters. However, this does not make it

impossible to compare the effects of S1R ligands *ex vivo*, as ligand-treated and non-ligand-treated samples were obtained in parallel from the same platelet population.

The effects of S1R ligands on eicosanoid synthesis in the abdominal aorta were very different from those observed in platelets. In the aorta of diabetic rats, we demonstrated reduced synthesis of 6-k-$PGF_{1\alpha}$ (Fig. 15B). In the aorta, NE-100 was shown to be the most potent S1R ligand in promoting the restoration of physiological status by enhancing 6-keto-$PGF_{1\alpha}$ synthesis. The increase in the total quantity of AA metabolites (COX+LOX) in the NE-100 group (Fig. 14B) suggests that this is probably due not only to specific prostacyclin synthase, but also to the effect of higher AA substrate due to phospholipase activation. In turn, *(S)*-L1 increases the rate of vasodilator COX products (Fig. 15B) by reducing the synthesis of vasoconstrictor, platelet aggregator eicosanoids in both vehicle-treated diabetic and vehicle-treated healthy rat aorta. In the study of AA metabolism in the aorta, PRE-084 was the least effective ligand, not affecting the synthesis of COX pathway products in either vehicle-treated healthy or vehicle-treated diabetic rats [30]. These results confirmed our hypothesis that *in vivo* sub-chronic S1R ligands can modulate both platelet and aortic AA metabolism *ex vivo*. Platelet and endothelial cell AA metabolism are known to differ significantly under healthy conditions. Platelets primarily synthesize the vasoconstrictor thromboxane, whereas endothelial cells primarily synthesize the vasodilator prostacyclin. The balance between these AA metabolites plays a crucial role in maintaining normal local circulation [32,47,90]. Overall, S1R ligands have opposite effects on platelet and aortic AA metabolism in diabetic rats. Our hypothesis that S1R ligands modulate abnormal AA metabolism in platelets and aortic rings of diabetic rats such that the physiological balance between them is restored has been confirmed.

SUMMARY

We have detected S1R in rat platelets, both at gene and protein level. The *in vitro* application of PRE-084 ligand, known as an S1R agonist, enhanced AA metabolism in non-activated platelets from healthy male rats. This effect was detected by radioactive substrate and ELISA. *In vitro*, under the effect of PRE-084, non-activated rat platelets synthesized more aggregating than anti-aggregating COX metabolites, leading to platelet activation. This finding was supported by the increased ADP- and AA-induced platelet aggregation in response to PRE-084. Sub-chronic intraperitoneal treatment with the S1R agonist known as PRE-084, antagonist NE-100, and a novel ligand, *(S)*-L1, induced *in vivo* platelet and aortic function changes that resulted in detectable *ex vivo* eicosanoid synthesis changes, despite the absence

of ligand in the study sample. In healthy rat platelets, none of the ligands induced changes in either S1R or COX mRNA levels; i.e., the difference in AA metabolism cannot be explained by the effect of ligands on S1R or COX enzyme transcription. The differential degree and/or direction of eicosanoid synthesis changes induced by *in vivo* treatment with each S1R ligand in platelets and aortas of healthy and diabetic rats suggest that ligands differentially affect not only PLase, COX and LOX but also the translation, synthesis, and or activation of each specific enzyme. S1R ligands induce changes in the physiological balance between platelets and endothelial cells lining the aorta with different effects (aggregating/vasoconstrictor and anti-aggregating/vasodilator) on eicosanoids to maintain or, in diabetes, restore the physiological balance. Despite the fact that *(S)*-L1, an S1R antagonist, has a binding position similar to NE-100, its effect on eicosanoid synthesis is, however, identical to that of the ligand PRE-084 or NE-100. Of the S1R ligands we tested, the new *(S)*-L1 proved to be the most potent. All this suggests that S1R ligands have high enzyme, cellular and tissue specificity.

The main findings of our studies are:

1. Rat platelets have a sigma-1 receptor.

2. PRE-084 (sigma-1 receptor ligand) enhances *in vitro* AA metabolism and ADP- and AA-induced aggregation of rat platelets.

3. *In vivo* treatment with PRE-084, NE-100 and *(S)*-L1 (a novel) ligand induces changes detectable *ex vivo* in AA metabolism in platelets and aorta.

4. S1R ligands promote the restoration of the balance between platelet- and endothelium-derived eicosanoids with opposite effects in STZ-induced diabetes.

5. S1R ligands have high enzyme, cellular and tissue specificity.

6. Under our test conditions, the new *(S)*-L1 ligand proved to be the most potent. However, despite the fact that the sigma-1 receptor antagonist has a binding position similar to NE-100, it cannot unambiguously be called an antagonist.

FUNDING

This work could not have been done without financial supporters such as the National Research, Development and Innovation Office of Hungary (GINOP-2.3.2-15-2016-00060, EFOP-3.6.2-16-2017-00006), and the Gedeon Richter Plc. Centenarial Foundation (2020/K/21/2503).

Sándor Váczi was supported by a scholarship from Gedeon Richter's Talentum Foundation.

ACKNOWLEDGEMENTS

First of all, I would like to thank my supervisor, Dr. Zsófia Mezei, who has supported my research career throughout and from whom I have learned a great deal over the past years. Without her guidance, this Ph.D. thesis would not have been possible.

I would also like to thank Prof. Dr. Gyula Szabó and Prof. Dr. Zoltán Rakonczay, the former and current heads of the Department of Pathophysiology, who have provided me with the opportunity to work in their institution.

I owe a special debt of gratitude to Prof. Dr. Mária Deli and her research group, especially Dr. Lilla Barna and Dr. Mária Mészáros, for their help with my experiments and for the opportunity for joint publications.

I am grateful to Prof. Dr. Botond Penke, Prof. Dr. Tamás Janáky, Dr. Lívia Fülöp and Prof. Dr. Gábor Rákhely for their great aid and support during my work.

I would also like to thank Dr. Imre Földesi and the staff at the Department of Laboratory Medicine, Dr. Rita Ónody, Dr. Andrea Siska, Anita Kis and Anikó Váradi, for their help in the aggregation experiments and in determining the laboratory parameters.

I likewise wish to thank Dr. Ferenc Tömösi, Dr. Ferenc Bogár and Dr. Krisztián Laczi for their help during my research and all the colleagues at the Department of Pathophysiology for their help during my doctoral years.

Last but not least, many thanks indeed to my family and friends.

REFERENCES

1. Aishwarya R, Abdullah CS, Morshed M, Remex NS, Bhuiyan MdS. Sigmar1's Molecular, Cellular, and Biological Functions in Regulating Cellular Pathophysiology. Front Physiol [Internet]. 2021 Jul 7 [cited 2022 Mar 16];12:705575. Available from: https://www.frontiersin.org/Articles/10.3389/fphys.2021.705575/full

2. Maurice T, Su TP. The pharmacology of sigma-1 receptors. Pharmacol Ther. 2009 Nov;124(2):195–206.

3. Bhuiyan MS, Tagashira H, Fukunaga K. Dehydroepiandrosterone-mediated stimulation of sigma-1 receptor activates Akt-eNOS signaling in the thoracic aorta of ovariectomized rats with abdominal aortic banding. Cardiovasc Ther. 2011 Aug;29(4):219–30.

4. American Diabetes Association. Diagnosis and classification of diabetes mellitus. Diabetes Care. 2014 Jan;37 Suppl 1:S81-90.

5. Zhang K, Zhao Z, Lan L, Wei X, Wang L, Liu X, et al. Sigma-1 Receptor Plays a Negative Modulation on N-type Calcium Channel. Front Pharmacol. 2017;8:302.

6. Penke B, Fülöp L, Szűcs M, Frecska E. The Role of Sigma-1 Receptor, an Intracellular Chaperone in Neurodegenerative Diseases. CN [Internet]. 2017 Dec 14 [cited 2022 Mar 14];16(1). Available from: http://www.eurekaselect.com/152746/Article

7. Aishwarya R, Abdullah CS, Morshed M, Remex NS, Bhuiyan MS. Sigmar1's Molecular, Cellular, and Biological Functions in Regulating Cellular Pathophysiology. Front Physiol. 2021;12:705575.

8. Ricciotti E, FitzGerald GA. Prostaglandins and Inflammation. Arterioscler Thromb Vasc Biol [Internet]. 2011 May [cited 2023 May 14];31(5):986–1000. Available from: https://www.ncbi.nlm.nih.gov/pmc/articles/PMC3081099/

9. Paes AM de A, Gaspar RS, Fuentes E, Wehinger S, Palomo I, Trostchansky A. Lipid Metabolism and Signaling in Platelet Function. In: Trostchansky A, Rubbo H, editors. Bioactive Lipids in Health and Disease [Internet]. Cham: Springer International Publishing; 2019 [cited 2022 Mar 16]. p. 97–115. (Advances in Experimental Medicine and Biology; vol. 1127). Available from: http://link.springer.com/10.1007/978-3-030-11488-6_7

10. Rosen DA, Seki SM, Fernández-Castañeda A, Beiter RM, Eccles JD, Woodfolk JA, et al. Modulation of the sigma-1 receptor–IRE1 pathway is beneficial in preclinical models of inflammation and sepsis. Sci Transl Med [Internet]. 2019 Feb 6 [cited 2022 Mar 16];11(478):eaau5266. Available from: https://www.science.org/doi/10.1126/scitranslmed.aau5266

11. Gao QJ, Yang B, Chen J, Shi SB, Yang HJ, Liu X. Sigma-1 Receptor Stimulation with PRE-084 Ameliorates Myocardial Ischemia-Reperfusion Injury in Rats. Chinese Medical Journal [Internet]. 2018 Mar 5 [cited 2022 Mar 16];131(5):539–43. Available from: https://journals.lww.com/00029330-201803050-00006

12. Nardai S, László M, Szabó A, Alpár A, Hanics J, Zahola P, et al. N,N-dimethyltryptamine reduces infarct size and improves functional recovery following transient focal brain ischemia in rats. Experimental Neurology [Internet]. 2020 May [cited 2022 Mar 16];327:113245. Available from: https://linkinghub.elsevier.com/retrieve/pii/S0014488620300765

13. Tagashira H, Matsumoto T, Taguchi K, Zhang C, Han F, Ishida K, et al. Vascular endothelial σ1-receptor stimulation with SA4503 rescues aortic relaxation via Akt/eNOS signaling in ovariectomized rats with aortic banding. Circ J [Internet]. 2013 [cited 2022 Mar 16];77(11):2831–40. Available from: https://www.jstage.jst.go.jp/Article/circj/77/11/77_CJ-13-0256/_article

14. Ha Y, Saul A, Tawfik A, Zorrilla EP, Ganapathy V, Smith SB. Diabetes accelerates retinal ganglion cell dysfunction in mice lacking sigma receptor 1. Mol Vis. 2012;18:2860–70.

15. Su TP, Su TC, Nakamura Y, Tsai SY. The Sigma-1 Receptor as a Pluripotent Modulator in Living Systems. Trends in Pharmacological Sciences [Internet]. 2016 Apr [cited 2022 Mar 16];37(4):262–78. Available from: https://linkinghub.elsevier.com/retrieve/pii/S0165614716000043

16. Wang J, Xu D, Shen L, Zhou J, Lv X, Ma H, et al. Anti-inflammatory and analgesic actions of bufotenine through inhibiting lipid metabolism pathway. Biomedicine & Pharmacotherapy [Internet]. 2021 Aug [cited 2022 Mar 16];140:111749. Available from: https://linkinghub.elsevier.com/retrieve/pii/S075333222100531X

17. American Diabetes Association. Diagnosis and Classification of Diabetes Mellitus. Diabetes Care [Internet]. 2014 Jan 1 [cited 2022 Mar 16];37(Supplement_1):S81–90. Available from: https://diabetesjournals.org/care/Article/37/Supplement_1/S81/37753/Diagnosis-and-Classification-of-Diabetes-Mellitus

18. Carrizzo A, Izzo C, Oliveti M, Alfano A, Virtuoso N, Capunzo M, et al. The Main Determinants of Diabetes Mellitus Vascular Complications: Endothelial Dysfunction and Platelet Hyperaggregation. IJMS [Internet]. 2018 Sep 28 [cited 2022 Mar 16];19(10):2968. Available from: http://www.mdpi.com/1422-0067/19/10/2968

19. Gremmel T, Frelinger A, Michelson A. Platelet Physiology. Semin Thromb Hemost [Internet]. 2016 Feb 29 [cited 2022 Jan 28];42(03):191–204. Available from: http://www.thieme-connect.de/DOI/DOI?10.1055/s-0035-1564835

20. Koupenova M, Clancy L, Corkrey HA, Freedman JE. Circulating Platelets as Mediators of Immunity, Inflammation, and Thrombosis. Circ Res. 2018 Jan 19;122(2):337–51.

21. Koupenova M, Livada AC, Morrell CN. Platelet and Megakaryocyte Roles in Innate and Adaptive Immunity. Circ Res. 2022;130(2):288–308.

22. Mancuso ME, Santagostino E. Platelets: much more than bricks in a breached wall. Br J Haematol [Internet]. 2017 Jul [cited 2022 Mar 14];178(2):209–19. Available from: https://onlinelibrary.wiley.com/doi/10.1111/Bjh.14653

23. van der Meijden PEJ, Heemskerk JWM. Platelet biology and functions: new concepts and clinical perspectives. Nat Rev Cardiol [Internet]. 2019 Mar [cited 2022 Jan 28];16(3):166–79. Available from: http://www.nature.com/Articles/s41569-018-0110-0

24. Yeung J, Li W, Holinstat M. Platelet Signaling and Disease: Targeted Therapy for Thrombosis and Other Related Diseases. Pharmacol Rev. 2018 Jul;70(3):526–48.

25. Gleim S, Stitham J, Tang WH, Martin KA, Hwa J. An eicosanoid-centric view of atherothrombotic risk factors. Cell Mol Life Sci. 2012 Oct;69(20):3361–80.

26. Stratmann B, Tschoepe D. Atherogenesis and atherothrombosis – focus on diabetes mellitus. Best Practice & Research Clinical Endocrinology & Metabolism [Internet]. 2009 Jun 1 [cited 2023 May 15];23(3):291–303. Available from: https://www.sciencedirect.com/science/Article/pii/S1521690X08001735

27. Poznyak A, Grechko AV, Poggio P, Myasoedova VA, Alfieri V, Orekhov AN. The Diabetes Mellitus-Atherosclerosis Connection: The Role of Lipid and Glucose Metabolism and Chronic Inflammation. Int J Mol Sci. 2020 Mar 6;21(5):1835.

28. Rollini F, Franchi F, Muñiz-Lozano A, Angiolillo DJ. Platelet Function Profiles in Patients with Diabetes Mellitus. J of Cardiovasc Trans Res [Internet]. 2013 Jun 1 [cited 2023 May 15];6(3):329–45. Available from: https://doi.org/10.1007/s12265-013-9449-0

29. Váczi S, Barna L, Laczi K, Tömösi F, Rákhely G, Penke B, et al. Effects of sub-chronic, in vivo administration of sigma non-opioid intracellular receptor 1 ligands on platelet and aortic arachidonate cascade in rats. Eur J Pharmacol. 2022 Jun 15;925:174983.

30. Váczi S, Barna L, Laczi K, Tömösi F, Rákhely G, Penke B, et al. Effects of sub-chronic, in vivo administration of sigma-1 receptor ligands on platelet and aortic arachidonate cascade in streptozotocin-induced diabetic rats. PLoS One. 2022;17(11):e0265854.

31. Váczi S, Barna L, Harazin A, Mészáros M, Porkoláb G, Zvara Á, et al. S1R agonist modulates rat platelet eicosanoid synthesis and aggregation. Platelets [Internet]. 2021 Oct 26 [cited 2022 Mar 16];1–10. Available from: https://www.tandfonline.com/doi/full/10.1080/09537104.2021.1981843

32. Mezei Z, Zamani-Forooshani O, Csabafi K, Szikszai B, Papp E, Ónodi Á, et al. The effect of kisspeptin on the regulation of vascular tone. Can J Physiol Pharmacol [Internet]. 2015 Sep [cited 2022 Mar 16];93(9):787–91. Available from: http://www.nrcresearchpress.com/doi/10.1139/cjpp-2015-0013

33. Jiang G, Mysona B, Dun Y, Gnana-Prakasam JP, Pabla N, Li W, et al. Expression, subcellular localization, and regulation of sigma receptor in retinal muller cells. Invest Ophthalmol Vis Sci. 2006 Dec;47(12):5576–82.

34. Zhang H, Lv M, Jia J, Zhao Z, Zhang L, Lai L, et al. Expression of the 78 kD glucose-regulated protein is induced by endoplasmic reticulum stress in the development of hepatopulmonary syndrome. Gene. 2014 Mar 1;537(1):115–9.

35. van Zijp HM, Barendrecht AD, Riegman J, Goudsmits JMH, de Jong AM, Kress H, et al. Quantification of platelet-surface interactions in real-time using intracellular calcium signaling. Biomed Microdevices. 2014 Apr;16(2):217–27.

36. Schrödinger. Schrödinger Release 2019-4; Schrödinger, LLC, New York, NY, 2019;

37. Roos K, Wu C, Damm W, Reboul M, Stevenson JM, Lu C, et al. OPLS3e: Extending Force Field Coverage for Drug-Like Small Molecules. J Chem Theory Comput. 2019 Mar 12;15(3):1863–74.

38. Furman BL. Streptozotocin-Induced Diabetic Models in Mice and Rats. Curr Protoc Pharmacol. 2015 Sep 1;70:5.47.1-5.47.20.

39. Dvorácskó S, Lázár L, Fülöp F, Palkó M, Zalán Z, Penke B, et al. Novel High Affinity Sigma-1 Receptor Ligands from Minimal Ensemble Docking-Based Virtual Screening. Int J Mol Sci. 2021 Jul 29;22(15):8112.

40. Abdel-Halim MS, Lundén I, Cseh G, Änggård E. Prostaglandin profiles in nervous tissue and blood vessels of the brain of various animals. Prostaglandins [Internet]. 1980 Feb [cited 2022 Mar 16];19(2):249–58. Available from: https://linkinghub.elsevier.com/retrieve/pii/0090698080900234

41. Kis B, Szabó CA, Pataricza J, Krizbai IA, Mezei Z, Gecse Á, et al. Vasoactive substances produced by cultured rat brain endothelial cells. European Journal of Pharmacology [Internet]. 1999 Feb [cited 2022 Mar 16];368(1):35–42. Available from: https://linkinghub.elsevier.com/retrieve/pii/S0014299999000242

42. Cryer B. Management of Patients with High Gastrointestinal Risk on Antiplatelet Therapy. Gastroenterology Clinics of North America [Internet]. 2009 Jun [cited 2022 Mar 16];38(2):289–303. Available from: https://linkinghub.elsevier.com/retrieve/pii/S0889855309000326

43. Mezei Z, Kis B, Gecse Á, Telegdy G, Ábrahám G, Sonkodi S. Platelet eicosanoids and the effect of captopril in blood pressure regulation. European Journal of Pharmacology [Internet]. 1997 Dec [cited 2022 Mar 16];340(1):67–73. Available from: https://linkinghub.elsevier.com/retrieve/pii/S0014299997014027

44. Sweeney JD, Hoernig LA, Michnik A, Fitzpatrick JE. Whole blood aggregometry. Influence of sample collection and delay in study performance on test results. Am J Clin Pathol. 1989 Nov;92(5):676–9.

45. Tóth O, Calatzis A, Penz S, Losonczy H, Siess W. Multiple electrode aggregometry: a new device to measure platelet aggregation in whole blood. Thromb Haemost. 2006 Dec;96(6):781–8.

46. Dugan G, O'Donnell L, Hanbury DB, Cline JM, Caudell DL. Assessment of Multiplate platelet aggregometry using citrate, heparin or hirudin in Rhesus macaques. Platelets. 2015;26(8):730–5.

47. Mezei Z, Váczi S, Török V, Stumpf C, Ónody R, Földesi I, et al. Effects of kisspeptin on diabetic rat platelets. Can J Physiol Pharmacol [Internet]. 2017 Nov [cited 2022 Mar 16];95(11):1319–26. Available from: http://www.nrcresearchpress.com/doi/10.1139/cjpp-2017-0036

48. Glennon RA, Ablordeppey SY, Ismaiel AM, el-Ashmawy MB, Fischer JB, Howie KB. Structural features important for sigma 1 receptor binding. J Med Chem. 1994 Apr 15;37(8):1214–9.

49. Schmidt HR, Betz RM, Dror RO, Kruse AC. Structural basis for σ1 receptor ligand recognition. Nat Struct Mol Biol. 2018 Oct;25(10):981–7.

50. Amer MS, McKeown L, Tumova S, Liu R, Seymour VAL, Wilson LA, et al. Inhibition of endothelial cell Ca^{2+} entry and transient receptor potential channels by Sigma-1 receptor ligands. Br J Pharmacol. 2013 Mar;168(6):1445–55.

51. Yadav S, Storrie B. The cellular basis of platelet secretion: Emerging structure/function relationships. Platelets. 2017 Mar;28(2):108–18.

52. Wysokinski WE, Tafur A, Ammash N, Asirvatham SJ, Wu Y, Gosk-Bierska I, et al. Impact of atrial fibrillation on platelet gene expression. Eur J Haematol. 2017 Jun;98(6):615–21.

53. Horstman LL, Jy W, Ahn YS, Zivadinov R, Maghzi AH, Etemadifar M, et al. Role of platelets in neuroinflammation: a wide-angle perspective. J Neuroinflammation. 2010 Feb 3;7:10.

54. Ghoshal K, Bhattacharyya M. Overview of Platelet Physiology: Its Hemostatic and Nonhemostatic Role in Disease Pathogenesis. The Scientific World Journal [Internet]. 2014 [cited 2022 Jan 28];2014:1–16. Available from: http://www.hindawi.com/journals/tswj/2014/781857/

55. Braun A, Vogtle T, Varga-Szabo D, Nieswandt B. STIM and Orai in hemostasis and thrombosis. Front Biosci (Landmark Ed). 2011 Jun 1;16:2144–60.

56. Varga-Szabo D, Braun A, Nieswandt B. STIM and Orai in platelet function. Cell Calcium [Internet]. 2011 Sep 1 [cited 2022 Dec 28];50(3):270–8. Available from: https://www.sciencedirect.com/science/Article/pii/S0143416011000728

57. Varga-Szabo D, Braun A, Nieswandt B. Calcium signaling in platelets. J Thromb Haemost. 2009 Jul;7(7):1057–66.

58. Ramström S. Arachidonic acid causes lysis of blood cells and ADP-dependent platelet activation responses in platelet function tests. Platelets. 2019;30(8):1001–7.

59. Hayashi T, Su TP. The potential role of sigma-1 receptors in lipid transport and lipid raft reconstitution in the brain: implication for drug abuse. Life Sci. 2005 Aug 19;77(14):1612–24.

60. Starr JB, Werling LL. σ-Receptor Regulation of [3H]Arachidonic Acid Release from Rat Neonatal Cerebellar Granule Cells in Culture. Journal of Neurochemistry [Internet]. 2002 Nov 23 [cited 2022 Mar 14];63(4):1311–8. Available from: http://doi.wiley.com/10.1046/j.1471-4159.1994.63041311.x

61. Tagashira H, Bhuiyan MS, Shioda N, Fukunaga K. Fluvoxamine rescues mitochondrial Ca2+ transport and ATP production through σ(1)-receptor in hypertrophic cardiomyocytes. Life Sci. 2014 Jan 30;95(2):89–100.

62. Weng TY, Tsai SYA, Su TP. Roles of sigma-1 receptors on mitochondrial functions relevant to neurodegenerative diseases. J Biomed Sci. 2017 Sep 16;24(1):74.

63. Pabba M, Wong AYC, Ahlskog N, Hristova E, Biscaro D, Nassrallah W, et al. NMDA receptors are upregulated and trafficked to the plasma membrane after sigma-1 receptor activation in the rat hippocampus. J Neurosci. 2014 Aug 20;34(34):11325–38.

64. Iñiguez MA, Punzón C, Nieto R, Burgueño J, Vela JM, Fresno M. Inhibitory effects of sigma-2 receptor agonists on T lymphocyte activation. Front Pharmacol. 2013;4:23.

65. Iyer KS, Dayal S. Modulators of platelet function in aging. Platelets. 2020 May 18;31(4):474–82.

66. Mezei Z, Kis B, Gecse A, Tajti J, Boda B, Telegdy G, et al. Platelet arachidonate cascade of migraineurs in the interictal phase. Platelets. 2000 Jun;11(4):222–5.

67. Lin YH, Brown JA, DiMartino C, Dahms I, Salem N, Hibbeln JR. Differences in long chain polyunsaturates composition and metabolism in male and female rats. Prostaglandins Leukot Essent Fatty Acids. 2016 Oct;113:19–27.

68. Hardy M, Lessire S, Kasikci S, Baudar J, Guldenpfennig M, Collard A, et al. Effects of Time-Interval since Blood Draw and of Anticoagulation on Platelet Testing (Count, Indices and Impedance Aggregometry): A Systematic Study with Blood from Healthy Volunteers. J Clin Med. 2020 Aug 4;9(8):E2515.

69. Koessler J, Hermann S, Weber K, Koessler A, Kuhn S, Boeck M, et al. Role of Purinergic Receptor Expression and Function for Reduced Responsiveness to Adenosine Diphosphate in Washed Human Platelets. PLoS One. 2016;11(1):e0147370.

70. Nguyen L, Lucke-Wold BP, Mookerjee SA, Cavendish JZ, Robson MJ, Scandinaro AL, et al. Role of sigma-1 receptors in neurodegenerative diseases. J Pharmacol Sci. 2015 Jan;127(1):17–29.

71. Sibbing D, Braun S, Jawansky S, Vogt W, Mehilli J, Schömig A, et al. Assessment of ADP-induced platelet aggregation with light transmission aggregometry and multiple electrode platelet aggregometry before and after clopidogrel treatment. Thromb Haemost. 2008 Jan;99(1):121–6.

72. Hwang DH. Characteristics of the formation of the platelet lipoxygenase product from endogenous arachidonic acid. Lipids. 1982 Dec;17(12):845–7.

73. Evangelista V, Manarini S, Di Santo A, Capone ML, Ricciotti E, Di Francesco L, et al. De novo synthesis of cyclooxygenase-1 counteracts the suppression of platelet thromboxane biosynthesis by aspirin. Circ Res. 2006 Mar 17;98(5):593–5.

74. Hu Q, Cho MS, Thiagarajan P, Aung FM, Sood AK, Afshar-Kharghan V. A small amount of cyclooxygenase 2 (COX2) is constitutively expressed in platelets. Platelets [Internet]. 2017 Jan 2 [cited 2022 Mar 16];28(1):99–102. Available from: https://www.tandfonline.com/doi/full/10.1080/09537104.2016.1203406

75. Broos K, Feys HB, De Meyer SF, Vanhoorelbeke K, Deckmyn H. Platelets at work in primary hemostasis. Blood Rev. 2011 Jul;25(4):155–67.

76. Krüger-Genge A, Blocki A, Franke RP, Jung F. Vascular Endothelial Cell Biology: An Update. Int J Mol Sci. 2019 Sep 7;20(18).

77. Neubauer K, Zieger B. Endothelial cells and coagulation - PubMed. Cell Tissue Res [Internet]. 2022 [cited 2023 Jun 12];387(3):391–8. Available from: https://pubmed.ncbi.nlm.nih.gov/34014399/

78. Henein MY, Vancheri S, Longo G, Vancheri F. The Role of Inflammation in Cardiovascular Disease. Int J Mol Sci. 2022 Oct 26;23(21):12906.

79. Csányi G, Leprán I, Flesch T, Telegdy G, Szabó G, Mezei Z. Lack of endothelium-derived hyperpolarizing factor (EDHF) up-regulation in endothelial dysfunction in aorta in diabetic rats. Pharmacol Rep. 2007 Aug;59(4):447–55.

80. Mitchell JA, Kirkby NS. Eicosanoids, prostacyclin and cyclooxygenase in the cardiovascular system. Br J Pharmacol. 2019 Apr;176(8):1038–50.

81. Thon JN, Italiano JE. Platelets: Production, Morphology and Ultrastructure. In: Gresele P, Born GVR, Patrono C, Page CP, editors. Antiplatelet Agents [Internet]. Berlin, Heidelberg: Springer Berlin Heidelberg; 2012 [cited 2022 Mar 16]. p. 3–22. (Handbook of Experimental Pharmacology; vol. 210). Available from: http://link.springer.com/10.1007/978-3-642-29423-5_1

82. Cimmino G, Golino P. Platelet Biology and Receptor Pathways. J of Cardiovasc Trans Res [Internet]. 2013 Jun [cited 2022 Mar 16];6(3):299–309. Available from: http://link.springer.com/10.1007/s12265-012-9445-9

83. Hayashi T, Su TP. Sigma-1 receptor chaperones at the ER-mitochondrion interface regulate Ca(2+) signaling and cell survival. Cell. 2007;131(3):596–610.

84. Lewis R, Li J, McCormick PJ, L-H Huang C, Jeevaratnam K. Is the sigma-1 receptor a potential pharmacological target for cardiac pathologies? A systematic review. Int J Cardiol Heart Vasc. 2020 Feb;26:100449.

85. Egan K, FitzGerald GA. Eicosanoids and the Vascular Endothelium. In: Moncada S, Higgs A, editors. The Vascular Endothelium I [Internet]. Berlin, Heidelberg: Springer; 2006 [cited 2022 Mar 5]. p. 189–211. (Handbook of Experimental Pharmacology). Available from: https://doi.org/10.1007/3-540-32967-6_6

86. Shi Y, Vanhoutte PM. Macro- and microvascular endothelial dysfunction in diabetes. J Diabetes. 2017 May;9(5):434–49.

87. Elsner M, Guldbakke B, Tiedge M, Munday R, Lenzen S. Relative importance of transport and alkylation for pancreatic beta-cell toxicity of streptozotocin. Diabetologia [Internet]. 2000 Nov 30 [cited 2022 Mar 16];43(12):1528–33. Available from: http://link.springer.com/10.1007/s001250051564

88. Eleazu CO, Iroaganachi M, Eleazu KC. Ameliorative Potentials of Cocoyam (*Colocasia esculenta* L.) and Unripe Plantain (*Musa paradisiaca* L.) on the Relative Tissue Weights of Streptozotocin-Induced Diabetic Rats. Journal of Diabetes Research [Internet]. 2013 [cited 2022 Mar 16];2013:1–8. Available from: http://www.hindawi.com/journals/jdr/2013/160964/

89. Valentovic MA, Alejandro N, Betts Carpenter A, Brown PI, Ramos K. Streptozotocin (STZ) diabetes enhances benzo(alpha)pyrene induced renal injury in Sprague Dawley rats. Toxicol Lett. 2006 Jul 14;164(3):214–20.

90. Szkudelski T. Streptozotocin–nicotinamide-induced diabetes in the rat. Characteristics of the experimental model. Exp Biol Med (Maywood) [Internet]. 2012 May [cited 2022 Mar 16];237(5):481–90. Available from: http://journals.sagepub.com/doi/10.1258/ebm.2012.011372

91. Friederich M, Hansell P, Palm F. Diabetes, Oxidative Stress, Nitric Oxide and Mitochondria Function. CDR [Internet]. 2009 May 1 [cited 2022 Mar 16];5(2):120–44. Available from: http://www.eurekaselect.com/openurl/content.php?genre=article&issn=1573-3998&volume=5&issue=2&spage=120

92. Gul M, Laaksonen DE, Atalay M, Vider L, Hänninen O. Effects of endurance training on tissue glutathione homeostasis and lipid peroxidation in streptozotocin-induced diabetic rats: Training and glutathione in diabetic rats. Scandinavian Journal of Medicine & Science in Sports [Internet]. 2002 Jun [cited 2022 Mar 16];12(3):163–70. Available from: http://doi.wiley.com/10.1034/j.1600-0838.2002.120307.x

93. Vaidya AR, Wolska N, Vara D, Mailer RK, Schröder K, Pula G. Diabetes and Thrombosis: A Central Role for Vascular Oxidative Stress. Antioxidants (Basel). 2021 Apr 29;10(5):706.

94. Goguadze N, Zhuravliova E, Morin D, Mikeladze D, Maurice T. Sigma-1 Receptor Agonists Induce Oxidative Stress in Mitochondria and Enhance Complex I Activity in Physiological Condition but Protect Against Pathological Oxidative Stress. Neurotox Res. 2019 Jan;35(1):1–18.

95. Scridon A, Perian M, Mărginean A, Vântu A, Gherţescu D, Fişcă C, et al. Streptozotocin-induced diabetes mellitus – a paradox of high intrinsic platelet reactivity and low *in vitro* platelet aggregation. Acta Endocrinol (Buchar) [Internet]. 2019 [cited 2021 Jun 11];15(1):46–51. Available from: https://www.ncbi.nlm.nih.gov/pmc/Articles/PMC6535314/